

**Vibro-Acoustic Modeling of a Commercial Vehicle  
to Reduce the Interior Noise Level**

by

**Gülşen Kamçı**

**A Thesis Submitted to the  
Graduate School of Engineering  
in Partial Fulfillment of the Requirements for  
the Degree of**

**Master of Science  
in  
Mechanical Engineering**

**Koc University**

**February 2009**

Koc University  
Graduate School of Sciences and Engineering

This is to certify that I have examined this copy of a master's thesis by

Gülşen Kamçı

and have found that it is complete and satisfactory in all respects,  
and that any and all revisions required by the final  
examining committee have been made.

Committee Members:

---

İpek Başdoğan, Ph. D. (Advisor)

---

Murat Sözer, Ph. D.

---

İlker Yılmaz, MS.c.

Date: 08.02.2009

## **ABSTRACT**

The interior noise inside the passenger cabin of automobiles can be classified as structure borne or airborne. In this study, the structure-borne noise which is mainly caused by the vibrating panels enclosing the vehicle was investigated. Excitation coming from the engine causes the panels to vibrate at their resonance frequencies and these vibrating panels cause a change in the sound pressure level (SPL) and undesirable booming noise. In order to improve the SPL in the cabin, it is critical to understand the dynamics of the vehicle and more importantly how it couples with the air inside the cabin. A combined usage of two methodologies was adopted in order to predict the sound pressure level inside the passenger cabin of a commercial vehicle under the effect of engine disturbances. Those methodologies are the Finite element method (FEM) for the structural analysis and the Boundary Element Method (BEM) for the acoustic analysis. The adopted FEM-BEM approach takes advantage of the Modal Acoustic Transfer Vector (MATV) algorithm that combines the Acoustic Transfer Vectors (ATV) with the normal structural velocity boundary conditions. MATV algorithm allows the calculation of acoustic contribution of each individual structural mode. This procedure uses a vector product to calculate the sound pressure and it is computationally very efficient. Another analysis which uses the ATV concept is Panel Acoustic Contribution Analysis (PACA). PACA enables the user to determine the contribution rate of each radiating panel to the noise level inside the cabin. The results of MATV and PACA analysis can be utilized to improve the design of the cabin components to eliminate the critical structural modes and also to reduce the contribution of the radiating panels to the interior noise level. Finally, the idea of using a Helmholtz resonator in the cabin was studied to reduce the sound pressure levels. A hole is placed on the bulkhead of the vehicle to make it behave as a Helmholtz resonator. The location and size of the hole were altered to see the effect of the hole dimensions and

position. First, the analysis was performed on a simple rectangular box to determine the optimum location and size of the hole. Then, the analysis was repeated on the vehicle model that was used throughout this thesis. The results show that the hole on the bulkhead behaves as a Helmholtz resonator and improves the SPL at certain frequencies. However, it introduces another cavity mode and this additional mode can make the SPL worse at other frequencies.

## ÖZET

Araç sürücü kabinindeki ses, yapıdan kaynaklanan ve havadan kaynaklanan ses olmak üzere ikiye ayrılır. Bu çalışmada, aracı çevreleyen panellerin titreşmesi nedeniyle oluşan yapıdan kaynaklanan ses türü araştırılmıştır. Motordan gelen tahrik panellerin rezonans frekanslarında titreşmesine neden olmakta ve bu titreşen paneller kabin içinde ses basınç seviyelerinde değişikliğe sebep olarak istenmeyen ses türünü ortaya çıkarmaktadır. Kabindeki ses basınç seviyesini iyileştirmek için, araç dinamiğini anlamak, daha da önemlisi kabindeki hava ile nasıl ilişkilendiğini anlamak çok önemlidir. Motordan gelen tahrikin etkisi altında kabindeki ses basınç seviyelerini incelemek için iki farklı yöntemin birleşimi kullanılmıştır. Bu yöntemler, yapısal model için Sonlu Elemanlar Metodu (FEM) ve akustik model için Sınır Elemanlar Metodudur (BEM). Birleşik FEM-BEM metodu Akustik transfer vektörleriyle panel hızlarını birleştiren Modal Akustik Transfer Vektör (MATV) algoritmasından yararlanmaktadır. Bu algoritma her bir yapısal modun ses basınç seviyesine olan katkısının hesaplanmasına olanak sağlar. Ayrıca vektör çarpımını kullanması nedeniyle oldukça verimlidir. Akustik Transfer Vektör kavramını kullanan bir diğer analiz ise Panel Akustik Katkı analizidir (PACA). Bu analiz, kabini çevreleyen her bir panelin kabin içi ses seviyesine olan katkısını hesaplanmasına olanak sağlar. MATV ve PACA analizlerinin her ikisi de kritik yapısal modların ve titreşen panellerin ses seviyesine olumsuz etkisini yok ederek kabin tasarımının iyileştirilmesinde kullanılabilir. Ayrıca, Helmholtz rezonatörünün ses basınç seviyesini azaltmak amacıyla kullanılması araştırılmıştır. Aracın orta paneline Helmholtz rezonatörü işlevi görmesi amacıyla bir delik açılmıştır. Deliğin yeri ve büyüklüğü değiştirilerek ses basınç seviyesi üzerindeki etkisi araştırılmıştır. Deliğin optimum yeri ve büyüklüğünü saptamak için, analiz ilk önce basit bir dikdörtgen modelde yapılmış, daha sonra araba modelinde tekrarlanmıştır. Sonuçlar, aracın orta paneline yerleştirilen deliğin Helmholtz rezonatörü gibi davrandığını ve belli

frekanslarda ses basınç seviyesini iyileştirdiğini göstermektedir. Fakat delik ek bir akustik mod yarattığı için diğer frekanslardaki ses seviyesinde kötüleşme görülmüştür.

## ACKNOWLEDGEMENTS

I would like to thank **Assist. Prof. İpek Başdoğan** (my advisor) for the chance of being a member of her research group, supplying us a productive and comfortable research environment and their support during my work. Also, I would like to thank my thesis committee members for their critical reading and useful comments.

I would like to thank also **İlker Yılmaz and Atayıl Koyuncu from Ford Otosan** for their financial support during my M.S. study.

I would like to thank my friends at Koç University; my former and recent office mates (**Erdem Yüksel, Ilgar Veryeri, Savaş Taşođlu, Çınar Ersanlı, Tolga Bayrak, Bekir Yenilmez, İsmail Filiz**), and also my beloved friend **Bekir Özbay** for their support, encouragement and good times during these 2 years.

And finally, I would like to thank **my family** for their continuous support and patience during every step of my education.

## TABLE OF CONTENTS

<b>Abstract</b> .....	iii
<b>Acknowledgements</b> .....	vii
<b>Table of Contents</b> .....	viii
<b>List of figures</b> .....	x
<b>List of tables</b> .....	xiii
<b>Nomenclature</b> .....	xiv
<b>Chapter 1 Introduction</b> .....	1
1.1 Structure borne/ airborne noise problems.....	1
1.2. Coupled and uncoupled problems.....	1
1.3. Interior and/or exterior acoustic problems.....	4
1.4. Transient versus time-harmonic problems.....	4
1.5. Scattering versus radiation.....	4
1.6. High and Low Frequency Noise Problems.....	5
<b>Chapter 2 Literature Review</b> .....	7
<b>Chapter 3 Coupled and Uncoupled Analyses</b> .....	13
3.1 Structural Finite Element Model.....	15
3.2 The Cavity (Acoustic) Finite Element Model.....	17
3.3 Mesh Mapping.....	18
3.4 Engine Disturbances Model.....	19
3.5 The Uncoupled Analysis Process Flow.....	20
3.6 Surrogate Mesh.....	24
3.7 The Coupled Analysis Process Flow.....	26
3.8 The Theory of Uncoupled and Coupled Analysis .....	27
3.8.1 FEM/FEM Model for the Uncoupled Analysis .....	27



3.8.2. FEM/FEM Model for the Uncoupled Analysis:.....	28
3.8.3 The results of coupled and uncoupled analyses.....	29
3.9 The comparison of the simulation and experimental results.....	34
<b>Chapter 4 A Combined FEM/BEM Approach to identify the critical modes and panels.....</b>	<b>42</b>
4.1 Boundary element modeling (FE/BE analyses).....	43
4.1.1 ATV based technology.....	44
4.1.1.1 ATV Response Analysis.....	44
4.1.1.1.1 PACA Process Flow.....	46
4.1.2 Modal Acoustic Transfer Vector (MATV) Analysis.....	50
4.1.2.1 MATV Process Flow.....	53
4.1.3 The evaluation of the results of PACA and MATV.....	55
<b>Chapter 5 Application of the Helmholtz Rezonator concept to reduce the sound pressure level.....</b>	<b>56</b>
<b>Chapter 6 Discussion and Conclusion.....</b>	<b>74</b>
<b>Bibliography.....</b>	<b>77</b>
<b>Vita.....</b>	<b>80</b>

## LIST OF FIGURES

Figure 3.1- Flow chart showing the differences between the coupled and the uncoupled analysis.....	15
Figure 3.2 Structural Finite Element Model showing the engine mounts as the disturbance input locations .....	16
Figure 3.3 Cavity Finite Element Model.....	18
Figure 3.4 The Amplitudes of Engine Forces.....	20
Figure 3.5 The Uncoupled Analysis Process Flow.....	21
Figure 3.6 Spherical mesh (output points on it).....	22
Figure 3.7 Acoustic modal participation factors.....	24
Figure 3.8 The Surrogate mesh.....	25
Figure 3.9 The process involved in setting up the coupled method.....	26
Figure 3.10 Comparison of the results of two methods at the position of left ear.....	30
Figure 3.11 Comparison of the results of two methods at the position of right ear.....	31
Figure 3.12 SPLs of left ear according to direction of engine forces applied separately....	32
Figure 3.13 SPLs of left ear according to direction of engine forces applied simultaneously .....	33
Figure 3.14 Simulation results of the analyses performed at Ford Otosan A.S. and LMS Virtual Lab.....	35
Figure 3.15 Transfer functions for left mount engine force in x, y and z direction.....	36
Figure 3.16 Transfer functions for right mount engine force in x, y and z direction.....	37
Figure 3.17 Transfer functions for transmission mount engine force in x, y and z direction.....	38
Figure 3.18 Scaled transfer functions.....	40

Figure 3.19 Simulation results of the analyses performed in Ford Otosan A.S. and LMS Virtual Lab with scaled engine forces.....	41
Figure 4.1 Comparison of FEM/FEM and FEM/BEM results.....	42
Figure 4.2 PACA Process Flow Diagram.....	47
Figure 4.3 Panels on the cavity model.....	48
Figure 4.4 Panel Acoustic Contribution Analysis.....	49
Figure 4.5 The contribution of structural modes to the acoustic response.....	52
Figure 4.6 Modal Participation plot obtained from Modal-Based Force Response Analysis.....	53
Figure 4.7 MATV Process Flow Diagram.....	54
Figure 5.1 Helmholtz resonator.....	56
Figure 5.2 Three dimensional model for a rectangular box with a hole on the mid-panel.....	59
Figure 5.3 Sound pressure levels inside the box model.....	60
Figure 5.4 Model 1.....	60
Figure 5.5 Model 2.....	61
Figure 5.6 Model 3.....	61
Figure 5.7 Model 4.....	62
Figure 5.8 Model 5.....	62
Figure 5.9 The sound pressure levels due to the different locations of holes.....	63
Figure 5.10 Model 4_1.....	64
Figure 5.11 Model 4_2.....	64
Figure 5.12 Model 4_3.....	65
Figure 5.13 The sound pressure levels due to the modifications in model 4.....	66
Figure 5.14 The effect of a hole on the bulkhead in the simplified structural model.....	67
Figure 5.15 MATV results for the simplified structural model without a hole.....	68

Figure 5.16 MATV results for the simplified structural model with a hole.....	69
Figure 5.17 Acoustic modal participation factors for the model without a hole.....	70
Figure 5.18 Acoustic modal participation factors for the model with a hole.....	71
Figure 5.19 The result of Panel Acoustic Contribution Analysis without a hole.....	72
Figure 5.20 The result of Panel Acoustic Contribution Analysis with a hole.....	73

## LIST OF TABLES

Table 3.1 Acoustic modes.....	23
Table 3.2 Scale factors for necessary engine mounts.....	39
Table 4.1 Panel names according to different colors.....	48
Table 5.1 Geometry and material data used for the simulation.....	59

## NOMENCLATURE

$[K_a]$	Acoustic stiffness matrix
$[M_a]$	Acoustic mass matrix
$[C_a]$	Acoustic damping matrix
$\omega$	Natural frequencies of the structural model
$w$	Nodal displacements of the panels
$F_a$	The excitation vector for the acoustic domain
$F_s$	The excitation vector for the structural domain
$[K_s]$	Structural stiffness matrix
$[M_s]$	Structural mass matrix
$[C_s]$	Structural damping matrix
$\rho_0$	Density of air
$p$	Sound pressure
$ATV$	Acoustic transfer vector
$ATM$	Acoustic transfer matrix
$MATV$	Modal acoustic transfer vector
$v$	Panel velocities
$[\phi_n]$	The matrix of modal vectors, projected on the local normal direction of structure boundary surface
$MPSP$	Vector of the modal participation factors
$f$	Natural frequency of Helmholtz resonator
$c$	Sound speed
$S$	Section area of Helmholtz resonator's neck

$V$  The cavity (volume) of Helmholtz resonator  
 $L$  The length of Helmholtz resonator's neck

## Chapter 1

### INTRODUCTION

The reduction of vehicle interior noise has become one of the most important issues related to driving conveniences. There are many sources that may cause high peaks at the sound pressure levels inside the passenger cabin. These sources can be classified as structure-borne and airborne [1]. In this thesis, we will study the structure-borne noise which is mainly caused by the engine excitations. The excitation coming from the engine may cause any part of the body structure to vibrate and consequently a change in the sound pressure level (SPL), in other words undesirable booming noise which is generally seen in the low frequency range of 50-200 Hz, inside the passenger cabin.

There are many sources in a vehicle that may cause the interior noise and it is not always possible to predict the interior noise level accurately before the vehicle is actually manufactured and being tested on the road. Therefore, some modifications might be required in the vehicle to improve the interior noise level after it is being built and tested in real driving conditions. However, manufacturers aim to predict the interior noise of the vehicle by performing numerical simulations before the vehicle design is finalized. In this respect, numerical simulation becomes a valuable tool for the manufacturers in terms of cost reduction in addition to less consumption of time and effort.

There are different types of numerical prediction techniques for acoustic analyses [1, 2]. However, each of these techniques has limitations by being applicable for a particular



type of acoustic problem. Therefore, it becomes very critical to make an appropriate selection according to the type of the acoustic problem that is encountered. The following classifications are considered while determining the type of acoustic problem.

### **1.1. Structure borne/ airborne noise problems.**

The engine and its accessories, tire/road interaction and airflow over the vehicle are the fundamental excitation sources for the acoustic domain inside the vehicle [1]. They can be classified into two categories. The first one is the structure-borne noise which is caused by the excitation coming from the engine or the disturbances coming from the road through the tires and the suspension system. The second one is the air-borne noise which is caused by the airflow over the vehicle body. In this thesis, only the structure-borne noise, particularly the engine-caused noise, was investigated.

### **1.2. Coupled and uncoupled problems**

In acoustics, it is called “vibro-acoustic coupling interaction” whenever an elastic structure is completely or partly in contact with a fluid [2]. This concept refers to the influence of structure and fluid on each other. Acoustic pressure along the fluid-structure interface may create loading on the structure which influences the structural vibrations. Conversely, the structural vibrations may affect the acoustic pressure field. The strength of this vibro-acoustic coupling interaction is largely dependent on the geometry of the structure and the fluid domain as well as on the fluid and structural material properties and on the frequency of the dynamic disturbances. Depending on the strength of the mutual interaction, vibro-acoustic systems may be classified into uncoupled and coupled systems.

In uncoupled vibro-acoustic systems, the mutual vibro-acoustic coupling interaction between structure and the fluid components is accepted as a very weak coupling that it may

be neglected in the dynamics analyses of acoustic problems. This consideration yields two types of uncoupled vibro-acoustic systems. In the first type, it is assumed that only structure affects the fluid and the vibrations of the structural components create an acoustic pressure field in the fluid components. In the second type, pressure distributions along the structure-fluid interface cause vibrations in the structural components.

In coupled vibro-acoustic systems, the mutual vibro-acoustic coupling interaction between the structural and the fluid components can not be neglected. In these systems, it is assumed that the structural and the fluid components affect each other mutually in a strong way. Therefore, structural vibrations can not be regarded as independent excitations for fluid components or vice versa, which means all components must be considered as parts of one coupled system.

The strength of mutual coupling interaction is not always obvious. For example, an elastic structure with a high stiffness is surrounded by a low density fluid initially seems an uncoupled vibro-acoustic system. However, when the size of the fluid domain is taken into account, it is understood that an elastic structure enclosing a small acoustic cavity can be strongly influenced by the fluid pressure, even if the cavity is filled with a low-density fluid.

In this study, both coupled and uncoupled approaches were studied to investigate the sound pressure level performance of the vehicle under the effect of engine disturbances. More detailed information about these analyses will be given in chapter 3.

### **1.3. Interior and/or exterior acoustic problems**

In an interior acoustic problem, the sound field is determined in a bounded fluid domain which is surrounded by a closed, vibrating boundary surface [2, 3]. The determination of the acoustic pressure field in the interior of a car due to the vibrations of the closed car body, like in this study, is a typical example of an interior problem.

In an exterior acoustic problem, the sound field is determined in an unbounded fluid domain [2, 3]. External sound fields are caused by the vibrations of open or closed structures. The noise radiated by a vibrating engine block is a typical example of exterior acoustic problems. There might be a combined interior/exterior acoustic problems which includes the calculation of sound fields on both sides of a closed boundary surface.

### **1.4. Transient versus time-harmonic problems**

A transient problem consists of determining the time history of a sound field due to a non-periodic excitation of the system. However, the acoustic excitation has a periodic and harmonic nature in many noise control engineering applications. For such time-harmonic problems, the acoustic design may be confined to the analysis of the various frequency components of the steady-state acoustic response spectrum, disregarding the transient phenomena [2]. In this thesis, we have studied the time-harmonic problem since the engine forces vary as a function of the engine revolution per minute (rpm) which will be discussed in chapter 3.

### **1.5. Scattering versus radiation**

In scattering problems, an acoustic wave with certain acoustic characteristics hits on a surface and then the reflected sound field is calculated. In radiation problems, vibrating panels generate the acoustic waves and then the radiated sound field is determined [2]. In

this study, vibrating cabin panels excited by the engine mount forces cause the sound pressure field in the acoustic domain.

### **1.6. High and Low Frequency Noise Problems**

Based on their frequency range of application, numerical methods can be classified into low-frequency and high-frequency prediction techniques [1, 2]. The finite element method (FEM) and boundary element method (BEM) are the most appropriate numerical techniques for the low-frequency dynamic analyses of vibro-acoustic systems. These two methods can be used separately or together to perform the vibro-acoustic analyses for the prediction of low-frequency responses.

Statistical Energy Analysis (SEA) is used to analyze the high-frequency vibro-acoustic behavior. In this technique, the structure is partitioned into subsystems and the frequency range is separated into smaller frequency bands. It is aimed to find the averaged energy values of each subsystem in each frequency band.

In this study, we present an approach for predicting the interior noise level of a commercial vehicle under the effect of engine disturbances. The methodology presented in this thesis also identifies the problematic components and panels of the vehicle that contribute to the SPL at most. We will be focusing on the sound pressure level at low frequencies up to 100 Hz, to investigate the causes of the mid-speed boom that occurs around 2500-3000 rpm. We used a combined FEM-BEM approach in addition to FEM/FEM method for the determination for sound pressure levels inside the passenger cabin. The following chapter provides the literature review related to the numerical methods used to predict the vibro-acoustic problems. Chapter 3 presents the details of the coupled and uncoupled vibro-acoustic analysis. Both methods use the finite element

method for modeling the structural and acoustical domains to perform the vibro-acoustic analyses. Chapter 4 gives the details of the combined FEM/BEM approach to identify the critical modes and panels that contribute to the interior noise at most. Chapter 5 provides the application of the Helmholtz resonator concept to reduce the sound pressure levels. A hole on the bulkhead of the vehicle is created such that the luggage compartment behaves as the cavity of the Helmholtz resonator whereas the hole area can be considered as the neck of the resonator. Finally, the thesis is concluded and future work is discussed in Chapter 6.

## Chapter 2

### LITERATURE REVIEW

The low- and mid-frequency internal noise of vehicles has always been the interest of both manufacturers and customers over the past 40 years, and many papers on the subject have been written. It is particularly important that manufacturers can predict the noise at an early stage of a new design so that the gain of money, time and effort can be obtained due to decrease in prototype mistakes. Besides, customer awareness has increased in terms of the vibration and noise control in vehicle so that the noise levels have become one of the most important criterions regarding to driving convenience.

As mentioned in Chapter 1, this thesis focuses on the structure borne noise. One of the most fundamental papers about the structure-borne noise was presented by Dowell [3]. He studied the structure-borne noise analytically in terms of acoustic/structural coupling. He gave a general theory of noise transmission analysis and developed an efficient numerical method for computing acoustic natural modes and interior noise levels due to wall motion. This structural-acoustic coupling analysis was commenced by the study of Dowell and Voss [4] in which the effects of panel vibrations on acoustic cavities were investigated.

Another fundamental paper on this subject was represented by was Dowell et al. [5]. They studied the modal expansion of the uncoupled acoustic and structural modes to analyze the structure-acoustic coupling. They developed a comprehensive theoretical model for sound fields which are created by flexible wall resulting from exterior sound

fields. Their method includes an expansion of the normal modes of the cavity with its walls assumed to be rigid.

Another analytical study about the acoustic/structural coupling was represented by Kim and Lee [6]. They studied the structural-acoustic response of a vehicle passenger compartment in terms of the structural-acoustic modal coupling coefficients and modal parameters of the systems. Also, they investigated how the panels surrounding the cavity contribute to the reduction of the noise inside the cabin. Different from the previous papers (3, 4, 5), computer program package (ACSTAP) which integrates numerical (FEM) and experimental data to analyze the combined structural-acoustic systems was developed for the noise reduction and design modification. They also supported their proposed method by the experimental results. Following this study, another practical method has been proposed by Kim et al. [7] to identify the cause of noise peak and to simplify the noise reduction procedure. This method is considering only a few modes and coupling coefficients, which contributes to acoustic response at most. Boundary element model (BEM) can be also used separately or together with FEM during vibro-acoustic analyses. In addition to FEM and BEM, Nalor and Prebsch [1] overviewed Statistical Energy Methods (SEA). Their paper is such a comprehensive study that not only the low and mid frequency prediction techniques but also the high frequency prediction techniques were discussed in detail. FEM/SEA hybrid method, which is a new developed method, was also mentioned. Apart from the numerical techniques, this paper also provides informative explanations about types of mechanisms causing the noise inside the vehicle.

Many researchers studied the accuracy and the limitations of FE and BE methods and reported on this topic so far [8-15]. Suzuki et al. [8] performed BE method to overcome the noise problems inside a vehicle cabin. They developed a methodology to analyze the effect of the absorbent materials adhered to vibrating surfaces of the cabin walls.

Frey mann et al. [9] focus on the coupled systems and investigated fluid-structure interaction to predict the sound pressure levels for coupled systems. In a similar study by Paul and Hagiwara [9], FE method was used to simulate the fluid-structure coupling to investigate the interior noise of a vehicle. They analyzed the correlation between vibration of cabin walls and sound pressure level at the position of the ear of a vehicle driver/passenger.

Another study which investigates a fully coupled system using finite element formulation was represented Nefske et al. [11]. Beside, the capabilities of finite element method were illustrated by computing acoustic modes and resonant frequencies of passenger compartment, investigating the effect of flexible walls on the cavity acoustics, and analyzing some techniques to compute the panel-excited noise.

Marburg and his co-workers [12-16] investigated the vibro-acoustic response of the noise level inside the vehicle cabin and also developed techniques to optimize the design parameters based on the vibro-acoustic analysis.

Vlahopoulos [17] developed a boundary element method in solving the Helmholtz equation for acoustic analysis. His method uses the structural analysis results obtained in NASTRAN to predict the noise emitted from the vibrating structure. He introduced a new approach numerically treat the singularity problem inherent in the boundary element methodology for acoustics. A vehicle interior noise analysis and a transmission cover noise radiation analysis, which are two practical applications, were presented.



Liu et al. [18] created a vibro-acoustic model to predict the noise inside the tracked vehicles. They developed a rigid multibody model of the system in ADAMS to determine the interaction forces between the running track system and the chassis hull of a tracked vehicle. Then, Finite element (FE) and boundary element (BE) models of the chassis hull of the vehicle were created and adopted to perform the vibro-acoustic analysis.

Bregant et al. [19] modeled a 3D cavity representing the earth-moving machine cab in ANSYS. They performed A BEM coupled analysis in Virtual Lab. to evaluate the cab inner vibro-acoustic field. They also modified the structural parameters based on the results of a vibro-acoustic field optimization. Another study including BEM and FEM together in vibro-acoustic analyses has been presented by Citeralla et al [20]. They developed an integrated approach for an automobile vibro-acoustic analysis to assess, visualize and compare vibro-acoustic performance to pre-determined design targets, while identifying and quantifying the forces and sound sources responsible for the current behavior. This study has an importance in the literature because it emphasized that numerical methods could be used for the diagnosis of noise problems besides being used as a predictive tool.

The types of the acoustic problems were covered in detail (eg: coupled, uncoupled, interior, and exterior etc.) in another study by Desmet and Sas [2],. They also compared the advantages and disadvantages of the numerical methods such as Boundary Element Methods, Finite Element Methods and Statistical Energy Analysis.

Desmet and Vandepitte [21] described the use of finite element method for time harmonics acoustic problems. Besides the basic principles of finite element method, they proposed some mathematical definitions for an interior acoustic problem. Then, they

extended these formulas to solve exterior problems. They also discussed the main properties of this method in terms of advantages and limitations.

Desmet [22] has another paper that focuses on the boundary element methods which is another valuable technique for acoustic problems. Similar to his previous study, he describes the use of boundary element method for solving time-harmonic acoustic problems. After mentioning different types of boundary integral formulation, he discussed some general properties of this method and made a comparison between the boundary element and finite element method. Finally, he investigated the coupling of an acoustic boundary element model with a structural finite element model for solving coupled vibro-acoustic problems.

Pirk et al. [23] analyzed both of the low and high frequency vibro-acoustic behavior of the Brazilian Vehicle Satellite Launcher. For low frequency analyses, the coupling effect of finite element model and cavity model, which are used for structural vibrations and acoustic pressure respectively, were investigated. Due to the limitations of FE and BE method, SEA technique was used. In this technique, they modeled their vibro-acoustic system as a composition of weakly coupled subsystems.

Alia and Souli [24] focused on a particular type of boundary element method which is called Variational BEM (VBEM). In this paper, they investigated the weak structure-acoustic interaction and transient acoustic problem type. They compared the efficiency of this method with FEM and came to a conclusion that VBEM was computationally deficient because of involving full matrices in which the components were calculated from double surface integration.

All of the studies from [21] to [24] were based on the numerical predictions techniques used for particular interior noise problems. To remind an important point emphasized in the study of Citarella et al. [20], numerical methods can also be useful to diagnose the reasons/sources for the noise problems. For example, Herrin et al. [25] focused on a new technique called Acoustic Transfer Vector (ATV) which enables the contribution analyses to identify the problem sources. They studied on an engine model which is separated into several different components such as engine block, front cover, oil pan etc. This analysis arose from the idea of that each of these components vibrates and radiates sound very differently from the other parts of the engine. The objective of this study, which is based on the contribution analysis, is to understand how these different sound radiating components contribute to the overall sound, and also to find out the reason for their low or high contribution.

Related to the theory of ATV concept and ATV based applications, Tournour's paper [26] covers two different approaches of these techniques using some formulations derived from boundary element formulations. In addition to formulations, its applicability for car interiors was explained briefly.

## Chapter 3

### COUPLED AND UNCOUPLED ANALYSES

In this chapter, the details of the coupled and uncoupled vibro-acoustic analyses are presented. Both methods use the finite element method for modeling the structural and acoustical domains to perform the vibro-acoustic analyses [2].

The finite element method (FEM) is the most common numerical method used for solving engineering problems. In this method, first the original problem is transformed into an equivalent integral formulation. Then, variable distributions and the geometry of the continuum domain are approximated in terms of a set of shape functions. These shape functions are locally defined within small subdomains, in other words “finite elements”, of the continuum domain. With these two concepts, the original problem of finding the variables of a continuum domain is transformed into a problem of finding the variables at some nodal positions within each element, which means it is transformed into a set of algebraic equations [2].

Two different approaches, coupled and uncoupled FE analyses were used to investigate the sound pressure level performance of the vehicle under the effect of engine disturbances (See Figure 3.1). The *uncoupled vibro-acoustic analysis* does not consider the mutual coupling interaction between the structural and the fluid components. In this analysis, only one way of interaction is considered and structural components are regarded as independent force excitations for the fluid components. However, in the *coupled vibro-acoustic analysis*

approach, the mutual vibro-acoustic coupling interaction between the structural and fluid components is no longer negligible and the system is regarded as a coupled system.

The processes of two methods are shown in the Figure 3.1. Coupled method starts with developing the finite element model of the structure in ANSYS. After the modal analysis is performed in ANSYS, the structural mesh is imported into SYSNOISE to construct the surrogate and cavity model. A surrogate model is required in SYSNOISE to represent the structural model since the mesh size of the cavity model and the structural model does not match and a representative model is needed to import the modal analysis results to SYSNOISE. The cavity model represents the fluid properties of the air inside the passenger cabin. After the force disturbances are applied at the engine mounts, the coupled analysis is performed to predict the sound pressure level inside the cabin. Similar to coupled analysis, the uncoupled analysis starts with the construction of the structural finite element model of the vehicle. The uncoupled analysis assumes one-way interaction between the structure and the fluid. Forced response analysis is performed on the structure under the effect of engine disturbances. The velocity outputs of the frequency response analysis are used as the boundary conditions on the cavity model in the vibro-acoustic analysis.

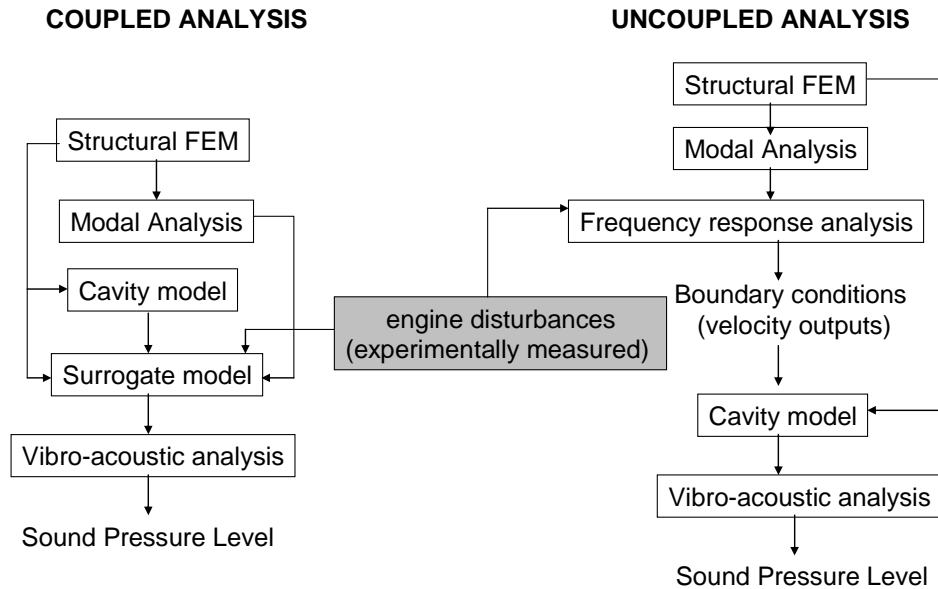


Figure 3.1 Flow chart showing the differences between the coupled and the uncoupled analysis

### 3.1. Structural Finite Element Model

Figure 3.2 shows the structural model used for uncoupled analysis.

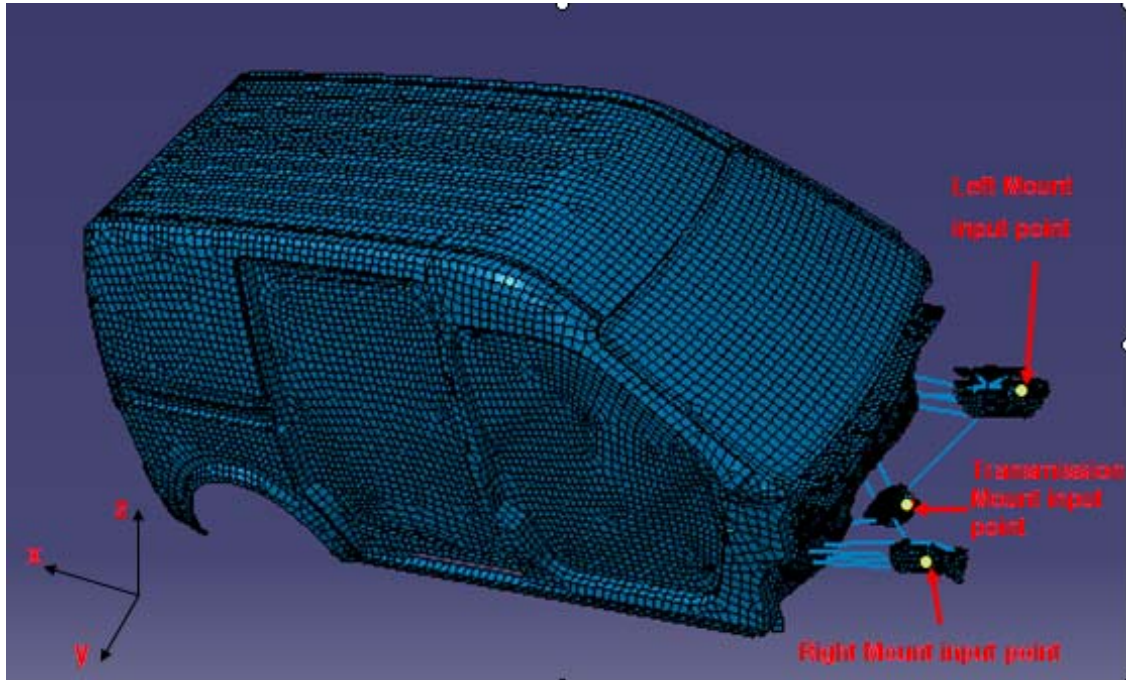


Figure 3.2 Structural Finite Element Model showing the engine mounts as the disturbance input locations

In this model, SHELL181 and MASS21 were used as element types. After determining the element types and identifying material properties, modal analysis was performed in the frequency range of 0-160 Hz. The analysis model only includes the hull system enclosing the cavities of the vehicle and the engine mounts are simply connected to the main body by welding. The main structure of the vehicle was modeled by using shell elements with different thicknesses. MASS 21 element type was used to represent the welding of the engine mounts to the main structure.

The forced response analysis for obtaining the velocity boundary conditions required for the uncoupled analysis was performed in the same frequency range (0-160 Hz) with an

interval of 1 Hz. The force disturbances, measured experimentally at the engine mounts, were used as the disturbance source for the structure. A global 1% structural damping was introduced. From the analysis, the velocities were obtained at every finite element node and then used as velocity boundary conditions in the uncoupled vibro-acoustic analysis.

### **3.2. The Cavity (Acoustic) Finite Element Model**

In order to analyze interior noise, the acoustic cavity of the vehicle needs to be both defined and meshed. As for any FE analysis it is important to create an accurate, realistic model. In order to analyze the interior noise, the interior (volume) should be meshed such that the vibration from the structure can be transferred to the cavity across the outer envelope of the cavity mesh.

Cavity mesh (volume mesh) was created directly from the structural finite element model in LMS Virtual Lab (SYSNOISE). The same cavity geometry seen below in the figure 3.3, which includes a mid-panel separating the cavity into two divisions, was used in all vibro-acoustic analyses including coupled and uncoupled analysis.



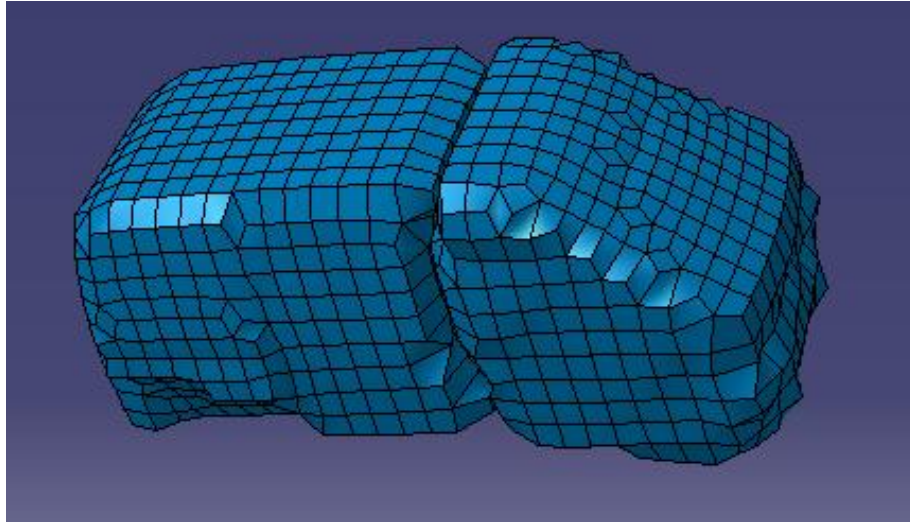


Figure 3.3 Cavity Finite Element Model

At first, the holes in the geometry are detected and repaired to define a cavity. The meshing algorithm mostly uses HEXA element type. In case of any disagreement between the structural and cavity mesh, it may add PENTA element type. That's why it is easy to handle sharp and smooth features. On the other hand, the size of the cavity mesh is determined by the user, which means the user has a great control on the cavity model.

### 3.3 Mesh mapping

As seen from figure 3.2 and figure 3.3, the structural and cavity meshes are quite incompatible. Therefore, a mesh mapping is required to link these incompatible meshes. The method used in Virtual Lab starts by creating automatically the envelope of the main cavity. Then, it is introduced to the software that every node on the envelope should be linked to the intended nodes on the structural mesh. Then, a distance value "Y" and a maximum number of nodes "X" on the structural mesh are defined, which means the software will generate a mesh mapping matrix on one node of the envelop mesh to

maximum  $X$  nodes on the structural mesh within a distance of  $Y$  mm. The nodes of the structural mesh that are linked to an acoustic node are called the wetted surface nodes. For the analyses in this thesis, distance was assigned as 50mm and the maximum node number was 4. This is normally sufficient to have a good coupling between the structural and acoustic mesh.

### **3.4 Engine Disturbances Model**

Engine forces are considered to be transferred to the structure at the mount application points. As it can be seen in the figure 3.2, there are three engine mount locations which are called left, right and transmission engine mounts. Each of them has three directions ( $x$ ,  $y$ ,  $z$ ) where the amplitudes may vary (see figure 3.5). Figure 3.5 shows the amplitude variation of the force data that is measured experimentally at the mount locations while the engine is running at different engine speeds. The study will be focusing on the causes of the mid-speed boom that occurs around 2500-3000 rpm. This rpm range corresponds to 93-100 Hz, because the engine is four-stroke engine, and on four-stroke engines, each cylinder is fired once for every two revolutions of the crankshaft, which means we should focus on 2<sup>nd</sup> harmonic force data.

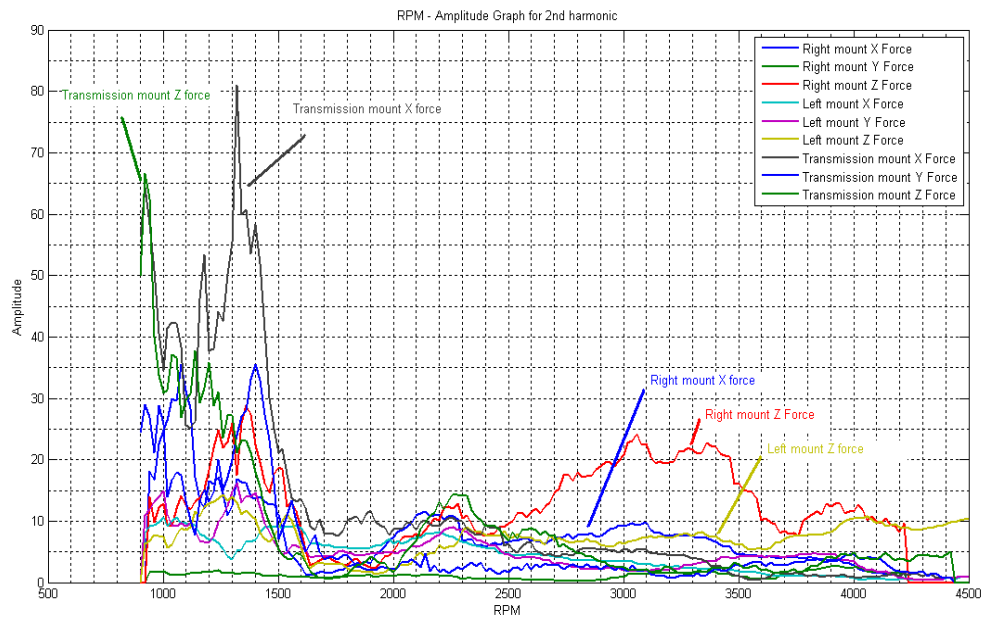


Figure 3.5 The amplitudes of engine forces

### 3.5. The Uncoupled Analysis Process Flow

The software LMS Virtual Lab. was used for performing all vibro-acoustic analyses. The steps followed in the uncoupled analysis can be seen in Figure 3.4.

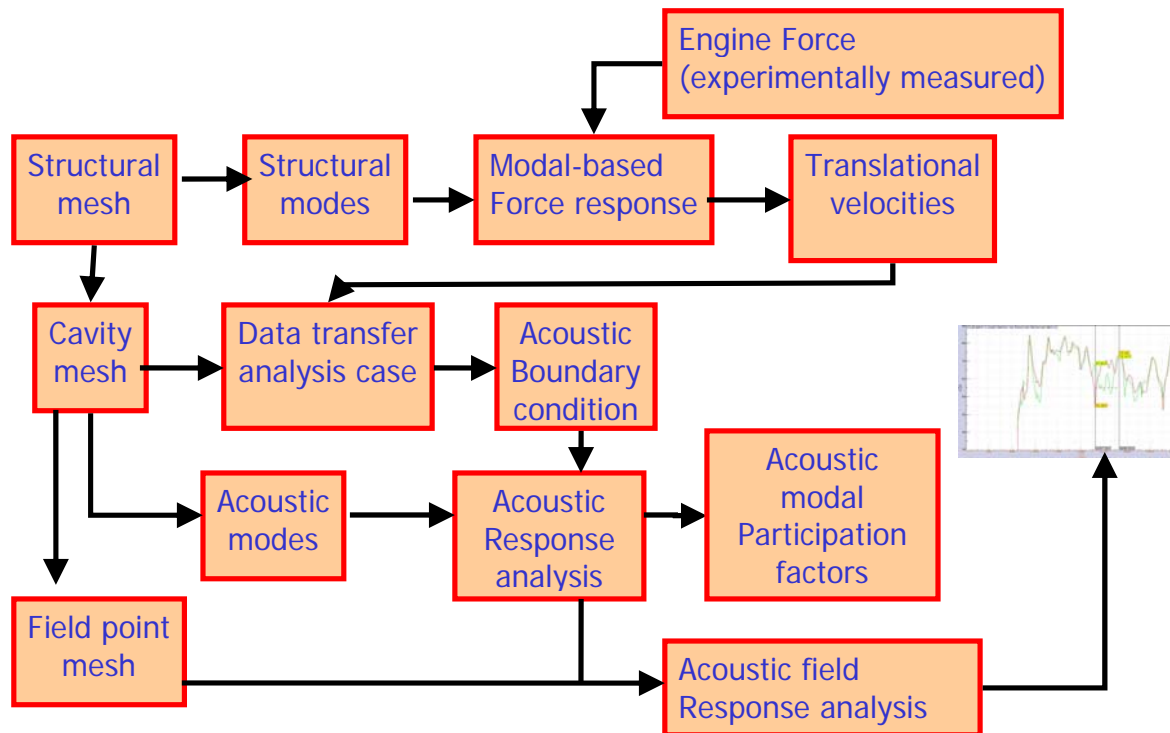


Figure 3.4 The Uncoupled Analysis Process Flow

Structural mode shapes and natural frequencies were calculated in the ANSYS. Then the result file, which includes the finite element geometry and mode shapes and natural frequencies, was imported to SYSNOISE and the engine forces were assigned to related mount locations. After assigning magnitudes and directions of force data to the related application points, a harmonic analysis called “Modal Based Force Response Analysis” was performed in SYSNOISE and as a result translational velocities of all nodes on the structural mesh were obtained.

After completing the structural analysis, some preparations should be done before the acoustic analysis. At first, cavity finite element model, seen in figure 3.3, was created from

structural finite element model in LMS Virtual Lab. Then a field point mesh (figure 3.6) representing the head of driver was created. As a final step before performing the acoustic analysis, boundary conditions should be designated for the cavity model. The translational velocities of each node on the structural mesh, which were obtained at the end of Modal-Based Force Response Analysis, were introduced as the boundary conditions for the acoustic domain.

After completing preparation steps, the acoustic analysis called “Acoustic Response Analysis Case” was performed. After that, sound pressure levels can be visualized for all locations in the cavity. As a last step, Acoustic field Acoustic Response Analysis was performed and sound pressure levels were obtained on the field mesh (figure 3.6), in other words at the location of the driver’s head.

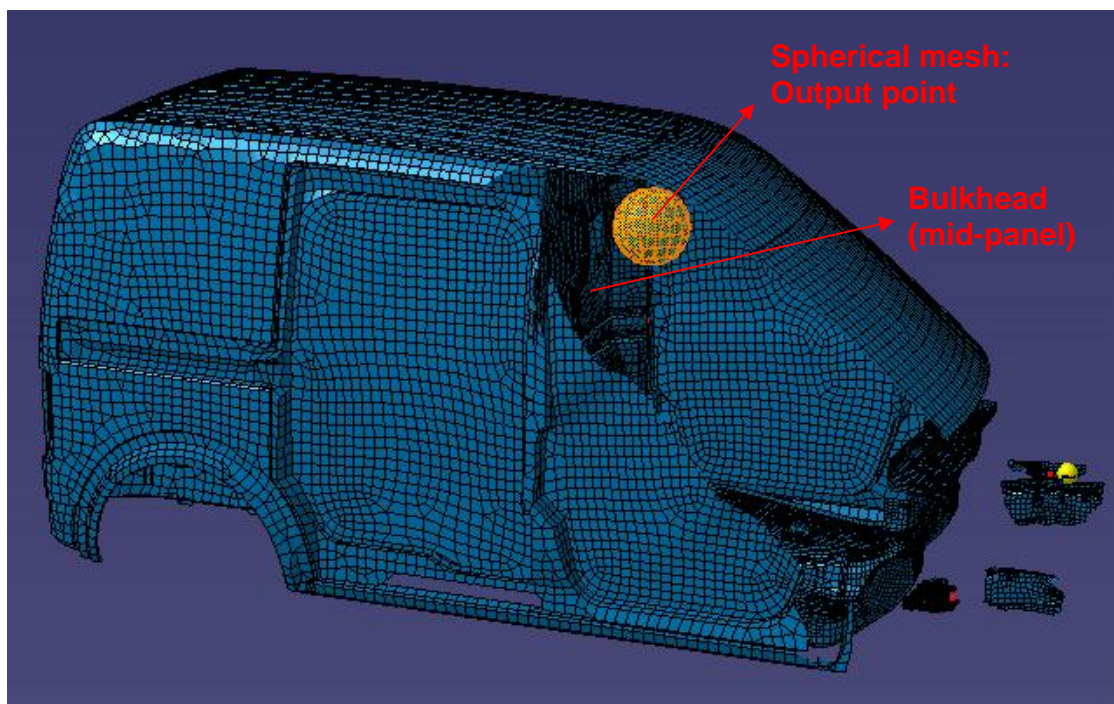


Figure 3.6 Spherical mesh (output points on it)

On the other hand, acoustic modal participation factors (see figure 3.7) that include the contribution of each acoustic mode to the sound pressure level can be visualized at the end of Acoustic Response Analysis Case. Acoustic modes are represented in table 3.1.

Mode number	Frequency (Hz)
1	0
2	0
3	92.991
4	113.182
5	118.093
6	121.281
7	127.145
8	149.989
9	151.91
10	158.6

Table 3.1 Acoustic modes

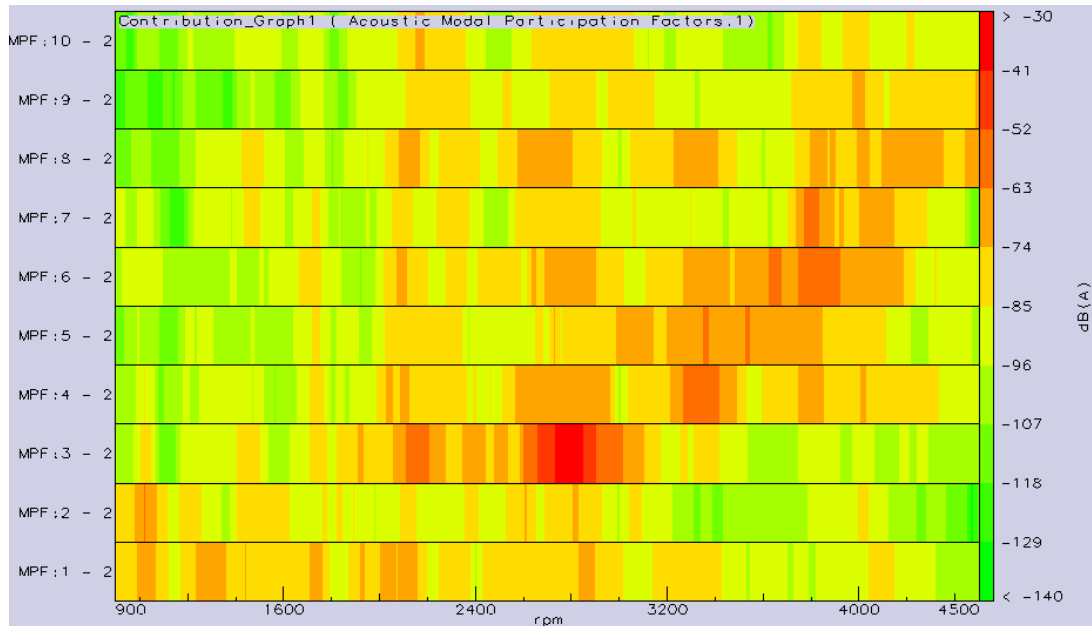


Figure 3.7 Acoustic modal participation factors

This figure shows the contribution of each acoustic mode (see table 3.1) to the sound pressure levels at different rpm values. Red color represents the maximum contribution, while the green color shows the least contribution. 3<sup>rd</sup> acoustic mode is the most influential mode between 2600 rpm and 3000 rpm. However, 3<sup>rd</sup> mode loses its importance above 3000 rpm and 4<sup>th</sup> and 5<sup>th</sup> acoustic modes become critical.

### 3.6 Surrogate Mesh

In a coupled vibro-acoustic analysis, the structural and the acoustic mesh need to be coincident at the wetted surface, where the cavity meets the structure. Generally the structural modes are calculated on a mesh that is very different and more detailed than the acoustic mesh. So a surrogate mesh that is compatible with the acoustic one at the wetted surface is needed. The structural modes will then be transferred on this coarser mesh.

The surrogate mesh seen below in figure 3.8 was used in the coupled analyses.

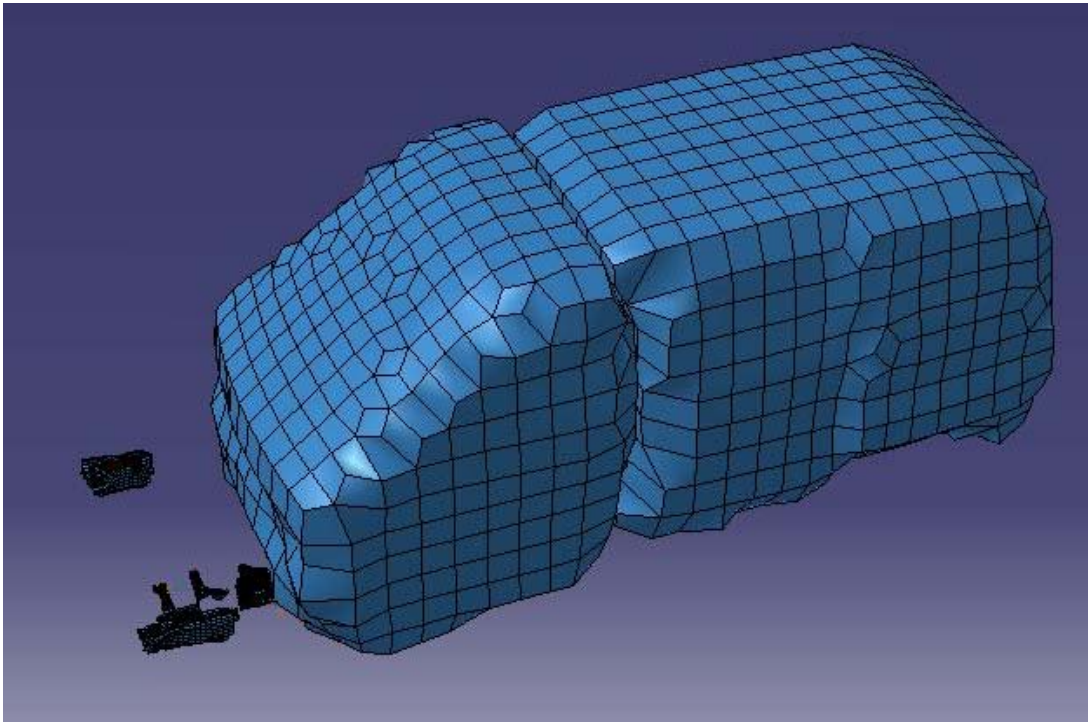


Figure 3.8 The Surrogate mesh

To create the surrogate mesh, first, the 3D cavity mesh (see section 3.2) should be generated. Then, only the skin mesh, in other word 2D mesh, of this volume mesh is scanned by a module in Virtual Lab. After having the shell elements of the cavity mesh, the engine mounts are taken from the structural mesh. Finally, cavity shell mesh and engine mount mesh are imported to LMS Virtual Lab at the same time and finally the surrogate mesh is obtained. These two meshes are not connected. They are just a collection of nodes and elements. There are no properties, materials or connections defined on the surrogate mesh since the structural behavior with the influence of all these parameters is coming



completely from the structural modes that were calculated on the detailed mesh. The surrogate mesh is simply a tool used to measure the influence of structural behavior on the acoustic results.

### 3.7 The Coupled Analysis Process Flow

All the steps followed in the coupled analysis can be seen below.

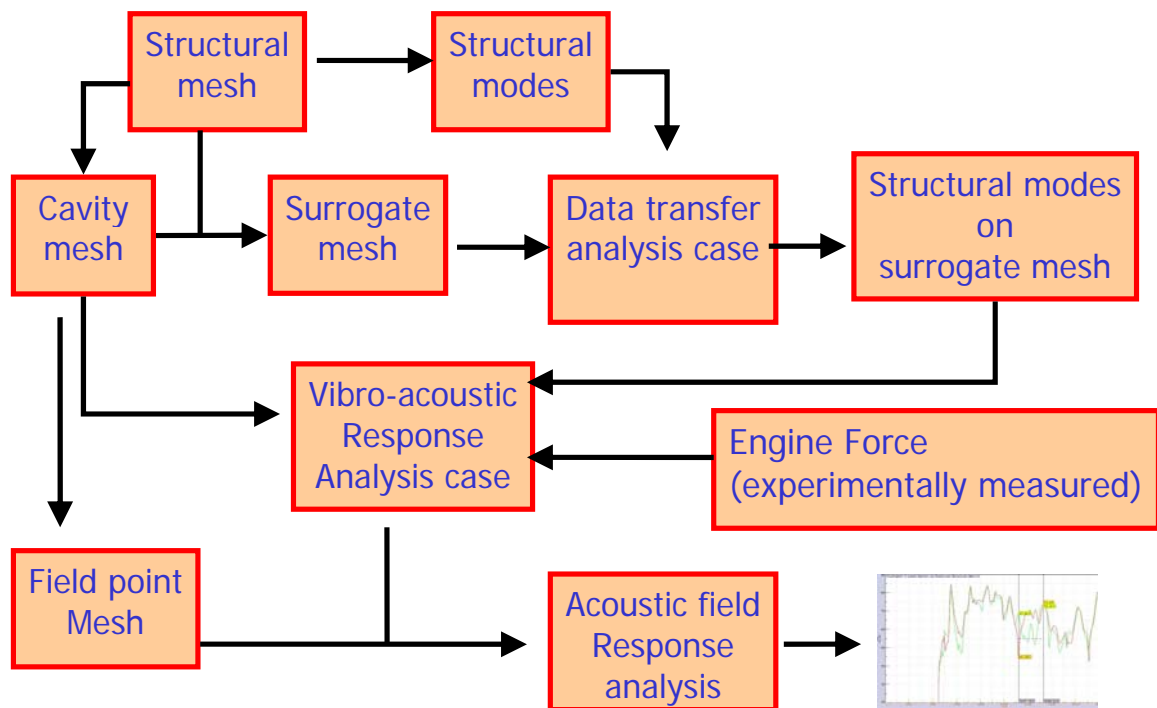


Figure 3.9 The process involved in setting up the coupled method

Similar to uncoupled analysis, for the beginning, model analysis was performed in ANSYS and structural modes were obtained. Different from the uncoupled analysis, Modal Based Force Response Analysis is not required to be performed for the coupled analysis. However, the original structural mesh should be modified to be compatible with the cavity

mesh. For this purpose surrogate mesh (see figure 3.8) was created like explained in the previous section. Since the surrogate mesh is just a combination of nodes and elements and does not include any properties or structural modes, a data transfer analysis case is necessary for transferring all information belonging to the original structural model. After performing data transfer analysis case, all structural modes were transferred on the surrogate mesh. After these preparation steps, acoustic analysis called Vibro-acoustic Response Analysis Case was performed. Finally, to visualize the results at intended points which are the field points mesh representing the driver's head, Acoustic Field Response Analysis was performed.

### 3.8 The theory of Uncoupled and Coupled Analysis:

Interior acoustic problems include a closed boundary surface. Three different types of boundary conditions, which are applied pressure, applied normal velocity, and normal impedance, may occur on this closed boundary surface [2, 21, 22]. In this thesis, only the applied normal velocity boundary condition is used for the acoustic domain.

#### 3.8.1 FEM/FEM Model for the Uncoupled Analysis

The uncoupled analysis solves the equations of the structural and acoustic models, separately. The structural response is described by the displacement vector. Structural finite element model of the uncoupled analysis can be written as [21]

$$\left( [K_s] + j\omega[C_s] - \omega^2[M_s] \right) \cdot \left\{ w_i \right\} = \left\{ F_s \right\} \quad (3.1)$$

The matrices  $[K_s]$ ,  $[C_s]$  and  $[M_s]$  are the structural stiffness, mass and damping matrices.  $\{w_i\}$  is the displacement vector.  $\{F_s\}$  contains the contributions coming from the engine as prescribed forces applied on the engine mounts.

The acoustic finite element model of the uncoupled problem is written as [21]

$$([K_a] + j\omega[C_a] - \omega^2[M_a]) \cdot \{p_i\} = \{F_{ai}\} \quad (3.2)$$

where  $[K_a]$ ,  $[C_a]$  and  $[M_a]$  are the acoustic stiffness, damping and mass matrices and  $\{p_i\}$  is the nodal pressure approximations obtained at the end of the vibro-acoustic analysis.  $\{F_{ai}\}$  contains the contributions from the input velocity vector obtained from equation 3.1. In this thesis, only the structural velocities obtained from the harmonic analysis were used as a boundary condition for the acoustic model, because there is not any acoustic source in our study. The uncoupled vibro-acoustic analysis considers one way interaction between the structure and the fluid.

### 3.8.2 FEM/FEM Model for the Coupled Analysis

In coupled vibro-acoustic model, the effect of the acoustic pressure on the elastic shell structure along the wetted surface (fluid-structural coupling interface) should be taken into account. For this purpose, the loading of the acoustic pressure on the structural finite element may be regarded as an additional load. As a result, the structural finite element model becomes

$$\left( [K_s] + j\omega[C_s] - \omega^2[M_s] \right) \cdot \left\{ w_i \right\} + [K_c] \cdot \left\{ p_i \right\} = \left\{ F_{si} \right\} \quad (3.3)$$

where  $[K_c]$  is the coupling matrix and  $\left\{ F_{si} \right\}$  is the new excitation vector after considering the effect of the acoustic pressure on the structural shell.

Combining the modified structural finite element model (3.3) and the acoustic finite element model (3.2) yields the Eulerian FE/FE model for an interior coupled vibro-acoustic system and can be written as [21],

$$\left( \begin{bmatrix} K_s & K_c \\ 0 & K_a \end{bmatrix} + j\omega \begin{bmatrix} C_s & 0 \\ 0 & C_a \end{bmatrix} - \omega^2 \begin{bmatrix} M_s & 0 \\ -\rho_0 K_c^T & M_a \end{bmatrix} \right) \cdot \begin{Bmatrix} w_i \\ p_i \end{Bmatrix} = \begin{Bmatrix} F_{si} \\ F_{ai} \end{Bmatrix} \quad (3.4)$$

The coefficients in the coupled stiffness matrix and coupled mass matrix are still frequency dependent; however these coupled matrices are no longer symmetric. Solution of these non-symmetric matrices requires non-symmetric equation solvers and as a result the coupled analysis takes more time when compared to the uncoupled analysis.

### 3.8.3 The results of coupled and uncoupled analyses

Initially, coupled and uncoupled analyses for only one engine mount force were performed to compare the differences between the results of the two methods. Left mount force in x direction was applied and the sound pressure levels were obtained at the position of the driver's left and right ears. The results can be seen below in figure 3.10 and 3.11.



Figure 3.10 Comparison of the results of two methods at the position of left ear



Figure 3.11 Comparison of the results of two methods at the position of right ear

As seen from figures 3.10 and 3.11, the results did not change significantly when those two methods were compared which gave an indication that the effect of the fluid on the structure can be neglected.

Although it seems there are more preparation steps before performing the acoustic calculation in uncoupled analysis, the computation time is less than the coupled analysis. Besides, in coupled analysis the surrogate mesh is the additional step because of the necessity of compatible meshes. Since the less difference in the SPL results and better calculation time, uncoupled method was chosen for the next analysis which will be performed to find out the most critical engine mounts. For this purpose, all engine forces were applied to the related mounts separately, which means that total of 9 uncoupled

analyses were performed due to the 3 engine mounts (left, right and transmission) and 3 force directions (x, y and z direction) on each mount. The following figure was obtained at the end of these analyses.

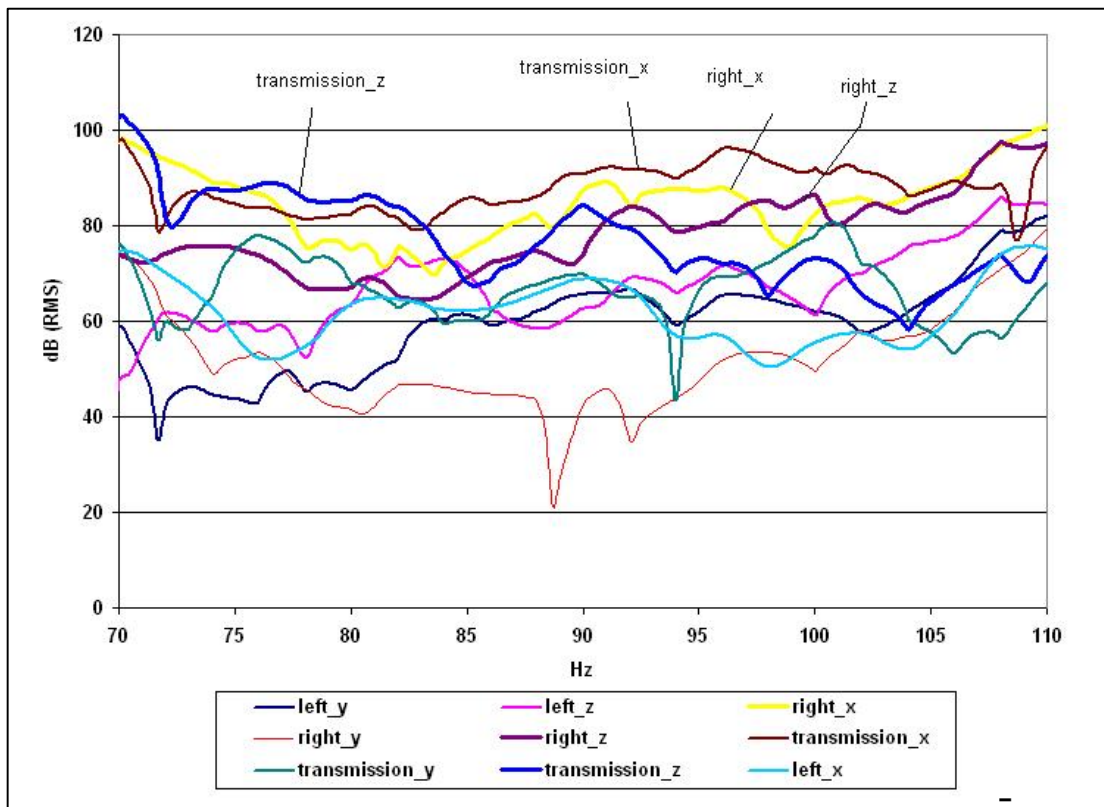


Figure 3.12 SPLs of left ear according to direction of engine forces applied separately

Figure 3.12 shows the contribution of each engine force on the sound pressure level. It can be observed that the forces acting on the transmission x and right x mounts contribute the most to the sound pressure level. After having this information, the analysis case where

only these two forces were applied to the structure was compared with the case where all the forces are applied at the same time (see figure 3.13). The results of those two cases are very similar which demonstrate that these forces (transmission x and right x) are the dominant ones in determining the sound pressure level of the cabin.

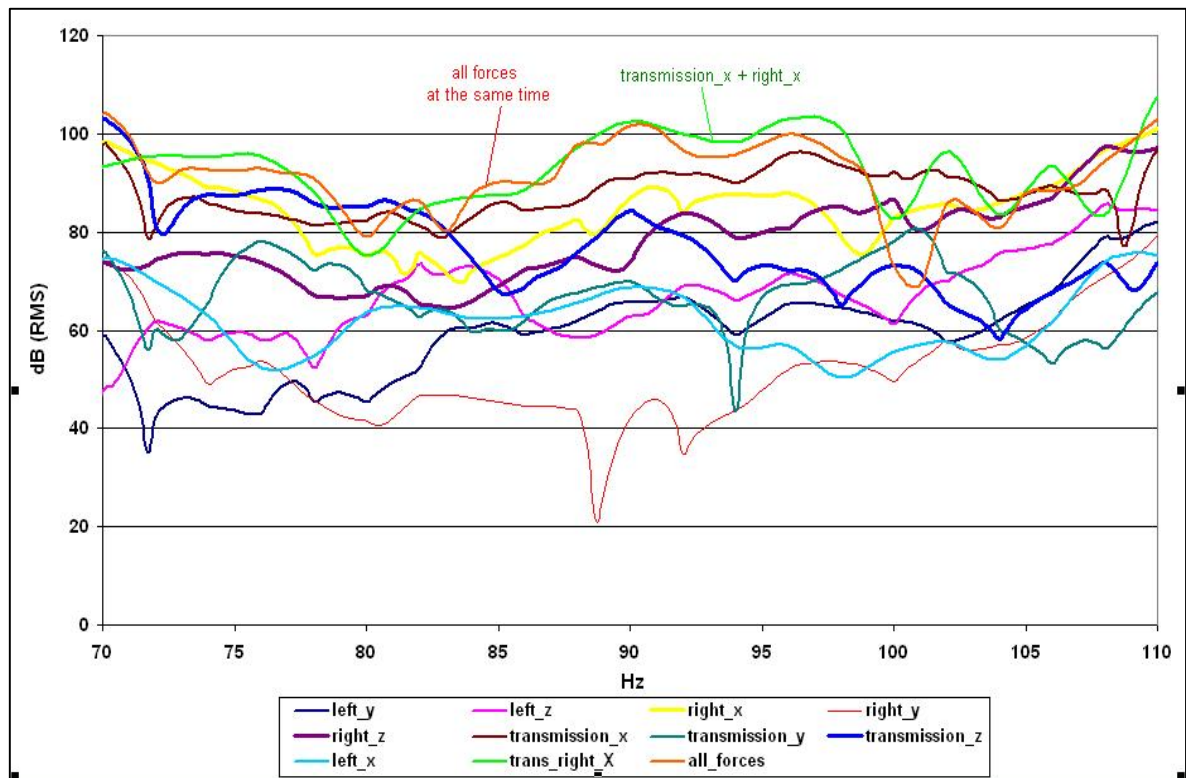


Figure 3.13 SPLs of left ear according to direction of engine forces applied simultaneously.

Although, figure 3.13 shows the sound pressure level as a function of engine speed, it is very difficult to identify the sources of the high peaks in this plot. We used two different approaches to identify the critical structural modes and the components of the structure which will be discussed in the following chapters.



### **3.9 The comparison of the simulation and experimental results**

It can be seen from figure 3.2 that the structural model which is used in all vibro-acoustic analyses is much simpler than the actual car model which is normally used by Ford Otosan. Their models include millions of degree of freedom which can not be handled by the computers that we have at Koç University. The simple model with nearly 30.000 degree of freedom was also generated at Ford Otosan to represent the actual model especially at the frequency range that is considered. The simple model includes only the external bulk model of the car cabin and the application points for the force data coming from the engine. As seen from the figure 3.2, there aren't any components between the body and the engine force application points. To make the model simple, these application locations were connected to the vehicle body rigidly. Because of all these simplifications, the simple structural model is expected to have different simulation results compared to the detailed Ford model. The difference can be seen clearly in the following figure.

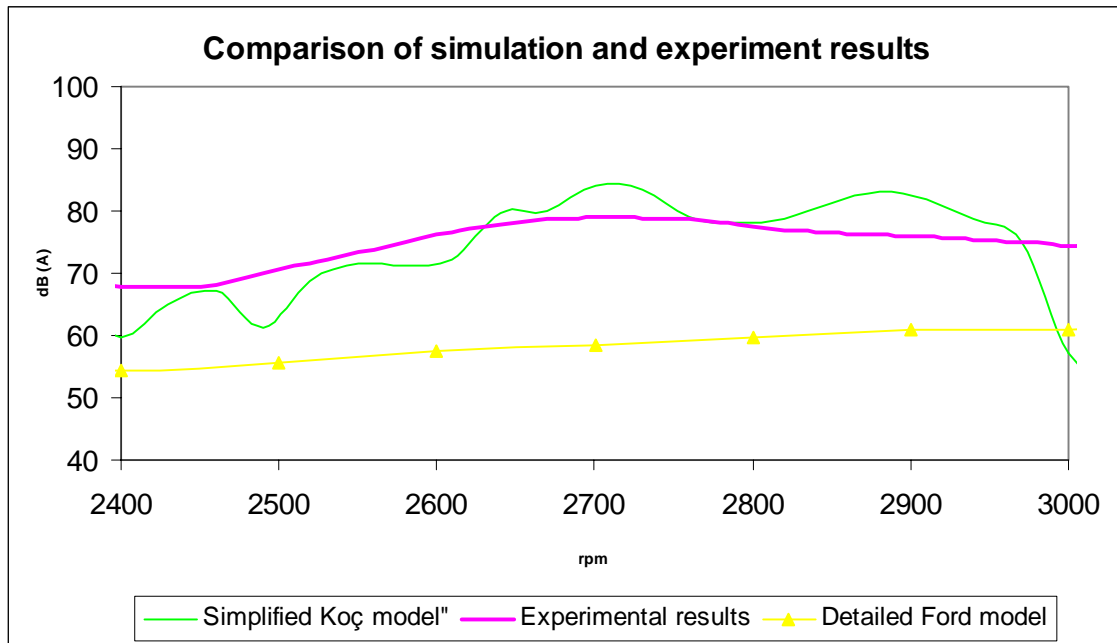


Figure 3.14 Simulation results of the analyses performed at Ford Otosan and LMS Virtual Lab.

The difference among two simulation results and experimental results was much more than expected. In order to identify the sources of the discrepancies between the two models, transfer functions for each engine mount were calculated (eg: The SPL is calculated under the effect of 1 N Force for each mount) using the detailed and the simple model and then compared with the measured transfer functions. (See figure 3.15-3.17). When the simulation results of the simple and detailed models are compared especially for the transmission x, y, right x and left z mounts, it is observed that the simplified model predictions are much different than the experimental measured ones. Even for the detailed model, it is observed that the model can not predict the peak values exactly. To make the simple model to be more representative to the detailed model, the force amplitudes are

scaled in the Forced Response Analysis to make the predictions more realistic. Table 3.2 summarizes the scaling factors used in the analysis.

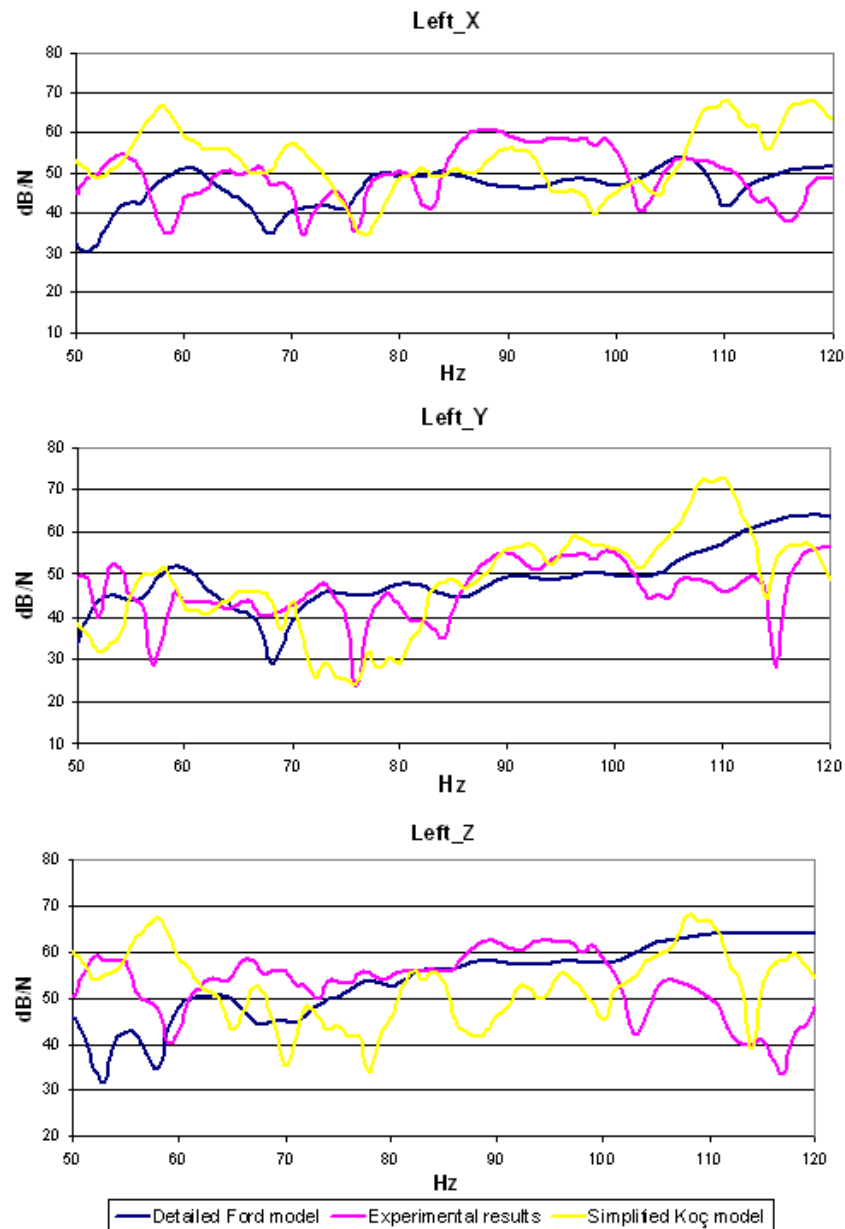


Figure 3.15 Transfer functions for left mount engine force in x, y and z direction

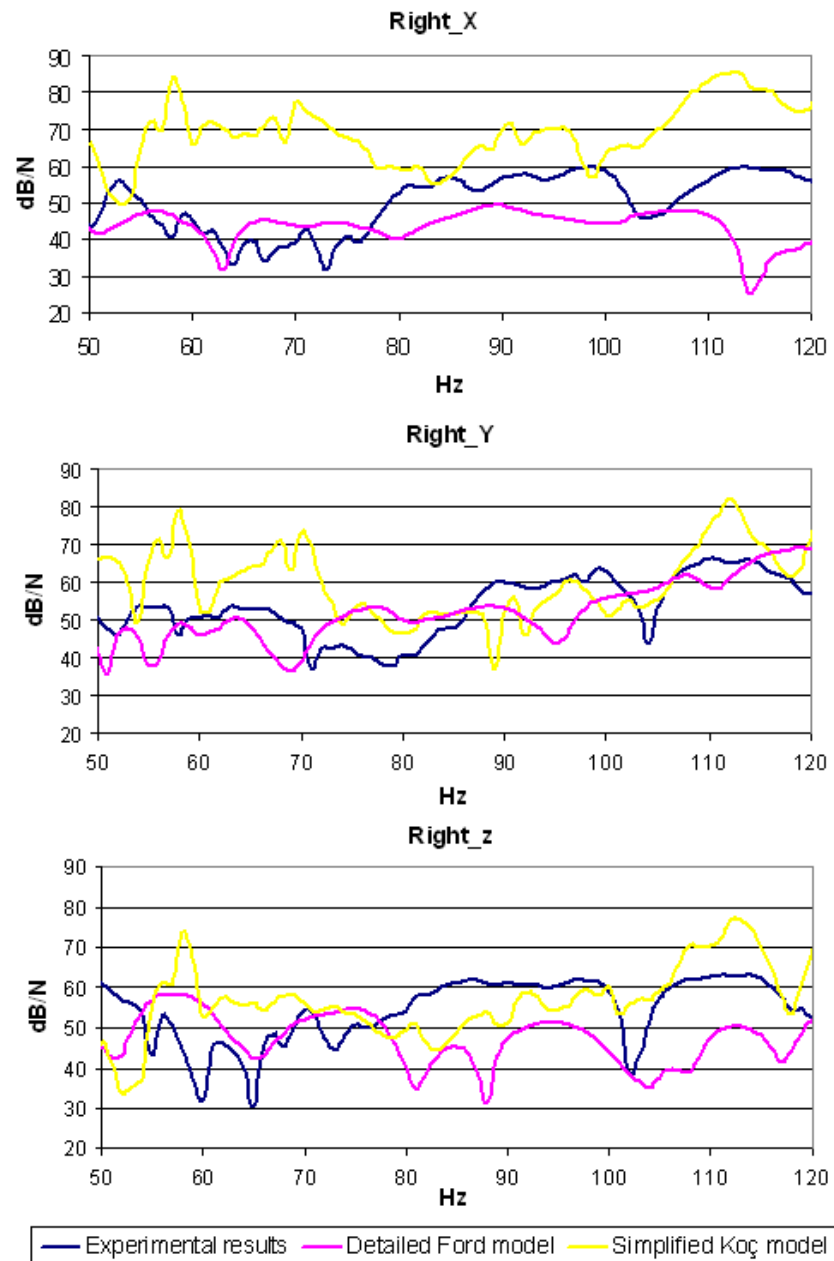


Figure 3.16 Transfer functions for right engine mount in x, y and z direction

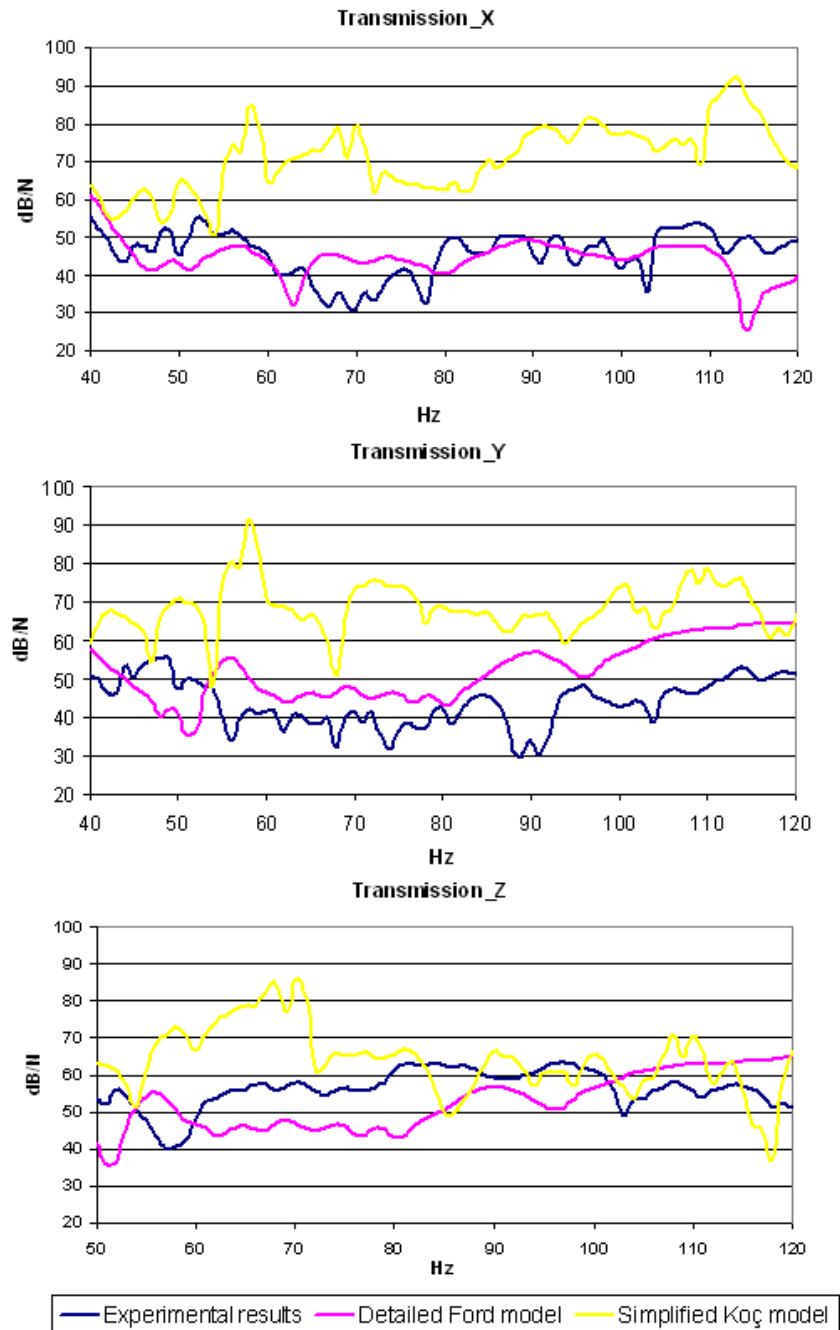


Figure 3.17 Transfer functions for transmission engine mount in x, y and z direction

---

<b>Engine mount</b>	<b>Scale factor</b>
Left _ z	1.9
Right _ x	0.4
Transmission _ x	0.05
Transmission _ y	0.3

Table 3.2 Scale factors

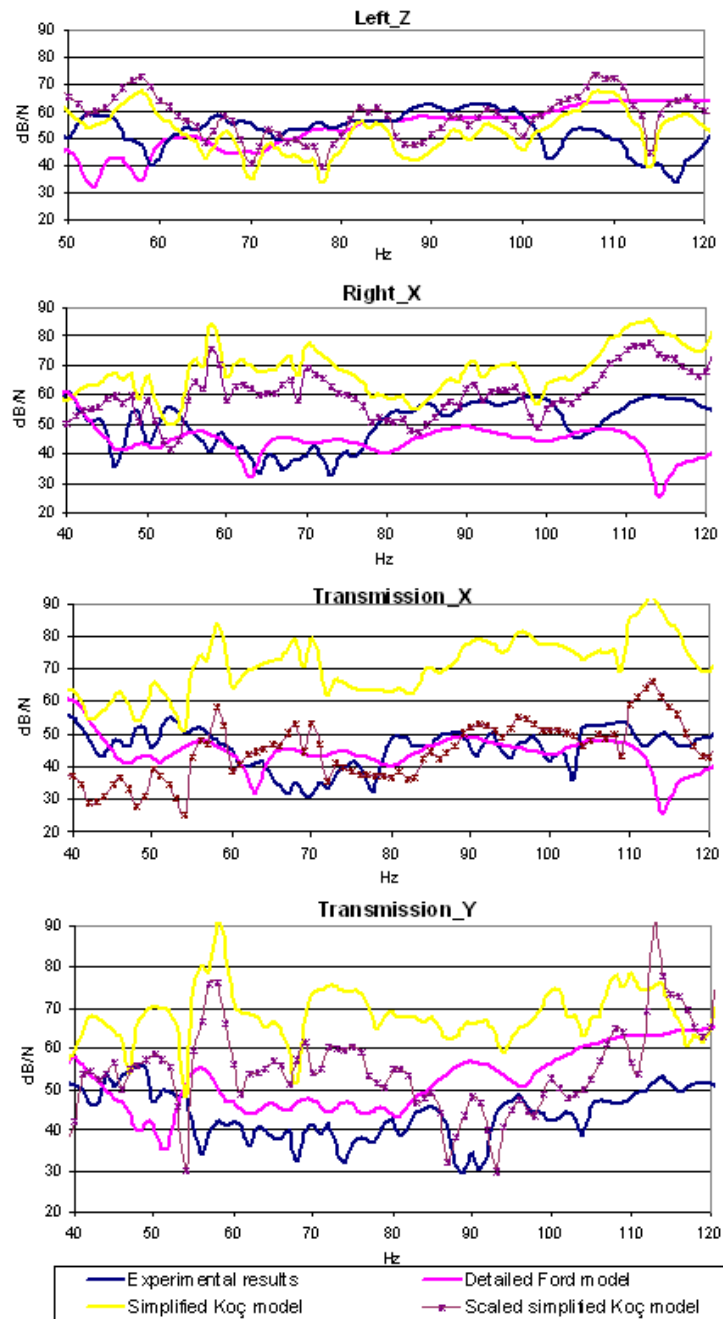


Figure 3.18 Scaled transfer functions

After determining the scale factors to make the transfer functions of the simple model similar with those of the actual model, sound pressure levels were recalculated and then compared with actual model's results.

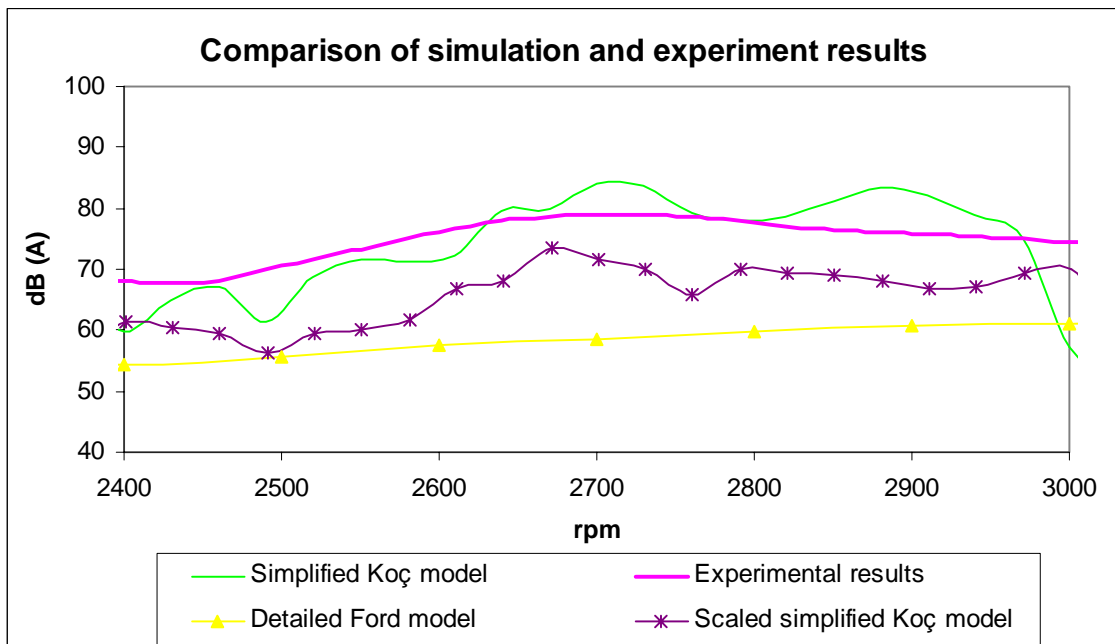


Figure 3.19 Simulation results of the analyses performed in Ford Otosan A.S. and LMS Virtual Lab with scaled engine forces.

As seen from the figure 3.19, the new results came closer to the simulation results of detailed model. However, we are on the conservative site since the simplified model results over bounds the detailed model results at all rpm range. Note that, the experimentally measured SPL should be higher than the predicted results. The experimental measurements are performed at the real driving conditions where wind, air intake, exhaust and road disturbances also contribute to the interior cabin noise. However, as we have described before, the predicted results only include the effect of the engine disturbances.



## Chapter 4

### A COMBINED FEM/BEM APPROACH TO IDENTIFY THE CRITICAL MODES AND PANELS

In the previous chapters, we calculated the SPL under the effect of the disturbances coming from the engine by using FEM/FEM method. This chapter gives the details of the combined FEM/BEM approach to identify the critical modes and panels that contribute to the interior noise at most. The combined FEM/BEM approach uses the boundary element method for calculating the pressure of the acoustic cavity. The results of the FEM/FEM and FEM/BEM approach were compared with each other (see figure 4.1).

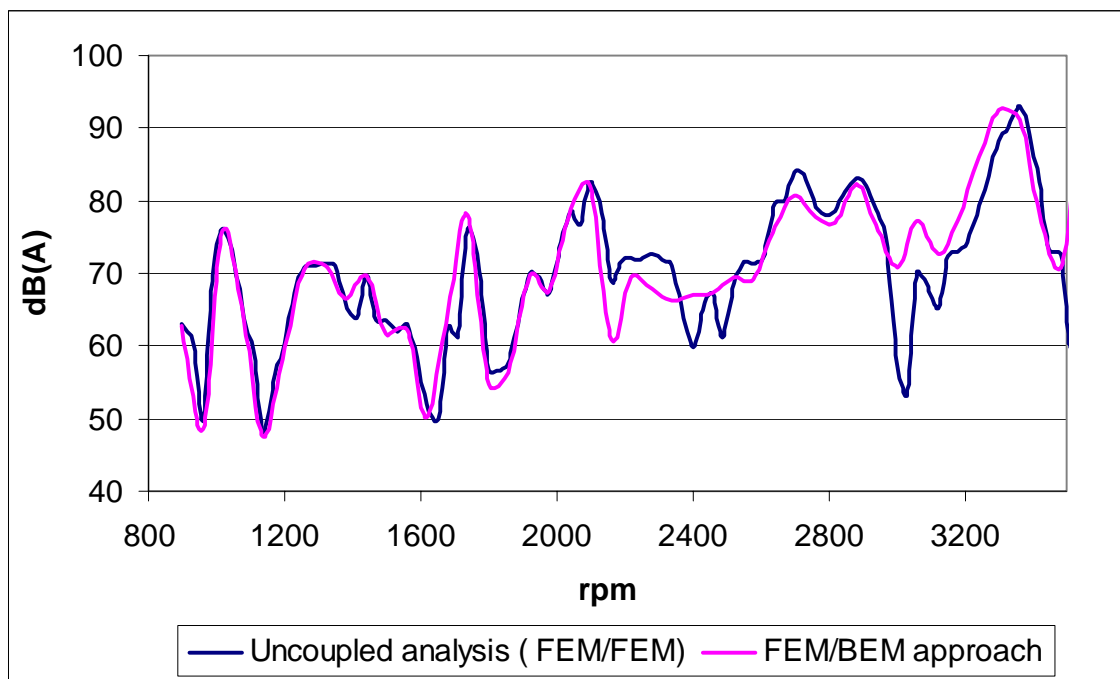


Figure 4.1 Comparison of FEM/FEM and FEM/BEM results

As it can be seen from figure 4.1, there is not a significant difference between the results of FEM/FEM and FEM/BEM approaches. However, FEM/BEM approach includes some advantages such as providing different types of analyses to identify the problematic modes and panels on the vehicle which will be discussed in the following sections. Considering these advantages, we decided to use FEM/BEM approach for the next analyses.

#### **4.1 Boundary element modeling (FE/BE analyses)**

The boundary element method is another common numerical method used for solving acoustic problems. Similar to the finite element model, a two-step procedure is followed in this method. In the first step, the original boundary problem is transformed into direct or indirect integral formulation. In the second step, boundary surface geometry and the boundary variables are approximated in terms of a set of shape functions, which are locally defined within small subsurfaces ('boundary elements') of the boundary surface [22].

Similar to finite element method, element concept is used to be able to transform the original problem, which is the determination of field variable distributions (sound pressures) inside the vehicle, into a problem of determining these field variables at some discrete positions within each boundary element.

The traditional BE and FE approaches use the structural vibrations directly to define the boundary conditions for the acoustic radiation problem. The draw back of this approach is that these boundary conditions vary with loading conditions and so a different solution must be found for each loading condition. In this thesis, a new approach called ATV based

technology, which is an integration method using the finite element and boundary element together, is presented.

#### 4.1.1 ATV based technology

ATV technology is based on Acoustic Transfer Vectors (ATVs) that link the input of the structural velocity of the radiating surface and the Sound Pressure Level at desired output field point [26].

$$\{\text{Sound Pressure}\} = \{\text{Acoustic Transfer Vector}\} \cdot \{\text{Surface Normal Velocity}\} \quad (4.1)$$

This method is tailored to make a more detailed analysis of the situation, to diagnose problems, to refine and improve the structural design. It provides extensive analysis data, and due to a particular methodology employed, that allows rapid and efficient re-runs to realize the optimum design. It will incorporate both the use of an FE solver to generate the structural modes and the BE solver for the generation of the acoustic internal radiation. Using this ATV technology, two different analyses which are ATV Response Analysis and Modal Acoustic Transfer Vector (MATV) Analysis were performed.

##### 4.1.1.1 ATV Response Analysis

ATV Response Analysis is also known as Panel Acoustic Contribution Analysis (PACA) which calculates the contribution of each panel to the sound pressure level inside the cabin. ATVs are combined with the modal-based forced response analysis results to calculate the contribution of each individual panel. The equation of PACA can be expressed as the following [26].

$$p(\omega) = \{ATV(\omega)\}^T \{v_n(\omega)\} \quad (4.2)$$

where  $p(\omega)$  is the sound pressure level at the position of driver's ear,  $v(\omega)$  represents the velocities of panels surrounding the cavity and  $ATV(\omega)$  shows the acoustic transfer vector between the input (the panels) and the output (the position of driver's ear).

The Acoustic Transfer Vectors from the radiating surface to specified field points are evaluated in the first step across the frequency range of interest at fixed frequency intervals. In the second step, the acoustic response in the field points is calculated for all loading conditions by combining the ATV with the normal structural velocity boundary condition vector at any frequency within the range. This ATV-response calculation is a vector-vector product, as given in equation 4.1.

This technique has an important advantage that the frequency dependent ATV's can also be used for contribution analysis, by a 'partial' vector-vector product only taking into account the normal velocity boundary conditions on part of the radiating surface,

$$p_c(\omega) = \{ATV(\omega)^e\}^T \{v_n(\omega)^e\} \quad (4.3)$$

where the superscript e denotes an element contribution. This way, the contribution of groups of elements, corresponding to distinct panels of the structure, can be derived.

ATVs in equation 4.2 and 4.3 are dependent only on the geometry and media characteristics of the acoustic domain, the acoustic surface characteristics, the frequency and the location of the output field points. They are independent of the loading and structural responses, which means that they are especially well suited for multi-case forced responses. The classical FE and BE approaches use the structural vibrations directly to define the boundary conditions for the acoustic radiation problem. The draw back of the

traditional approach is that the acoustic response must be calculated by solving the system equations for each loading condition. Since solving the equations for each load at each frequency is quite time consuming, ATV approach becomes more efficient in acoustic problems. First the acoustic transfer function is obtained from the radiating surface to the specific output field point for the predetermined frequency range. The loading condition is not taken into account in the first step, the step of calculation ATVs, because ATVs are independent of loading. In the following steps, structural velocities (indirectly loading) are introduced to the model as the boundary conditions, but ATVs doesn't change even if velocities vary due to different loading conditions. ATVs have different values only if output field points, in other words the positions of microphones, change. Other advantage of ATV technology is its convenience for structural design and optimization, because it is totally independent from geometry which allows fast re-runs for optimization [22, 26].

#### **4.1.1.1.1 PACA Process Flow**

The steps followed in this analysis can be seen below.

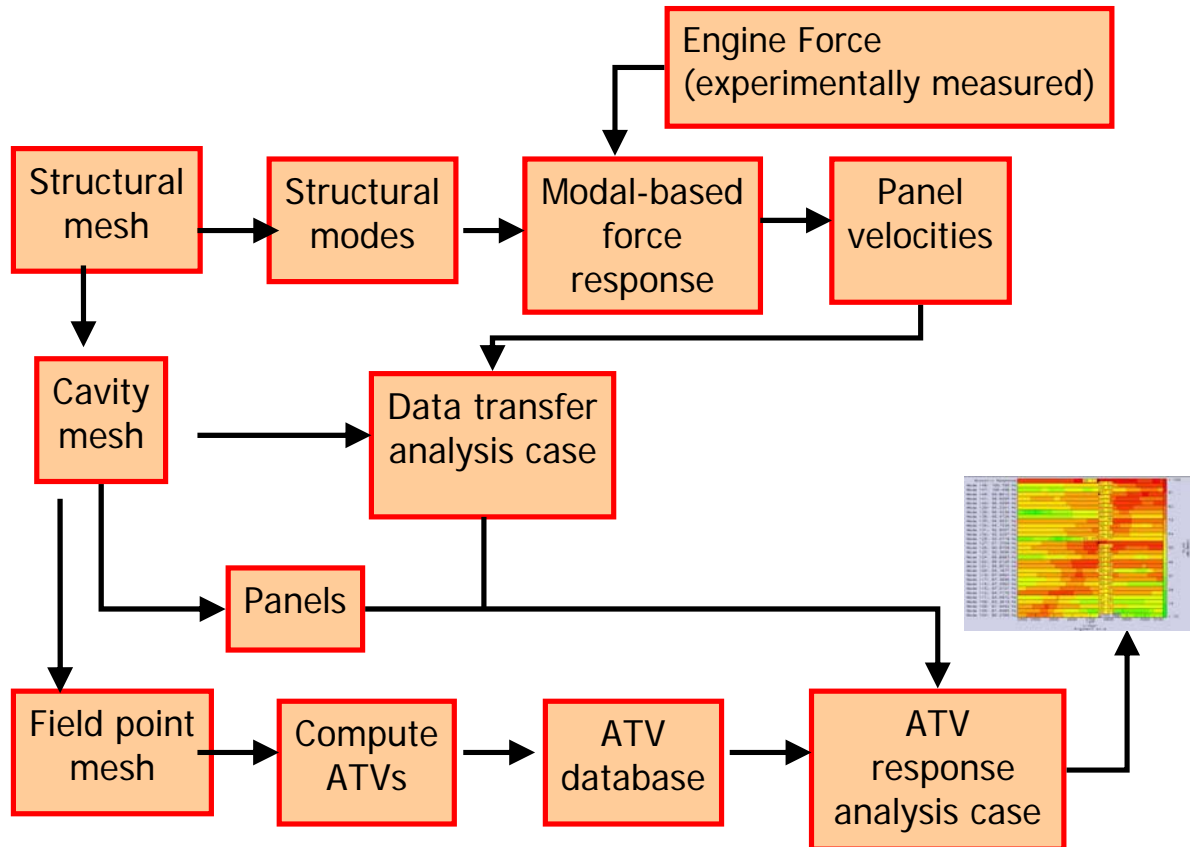


Figure 4.2 PACA Process Flow Diagram

As seen from the figure 4.2, there are some similarities with the steps of the previous analyses. For example, at first the structural modes were calculated in Ansys and then the harmonic analysis which is called Modal Based Force Response Analysis was performed and as a result the panel velocities were obtained. Cavity mesh was created like in the coupled and uncoupled analysis using the mesh generation module in LMS Virtual Lab. Differently; panels were created on the cavity mesh as seen in figure 4.3.

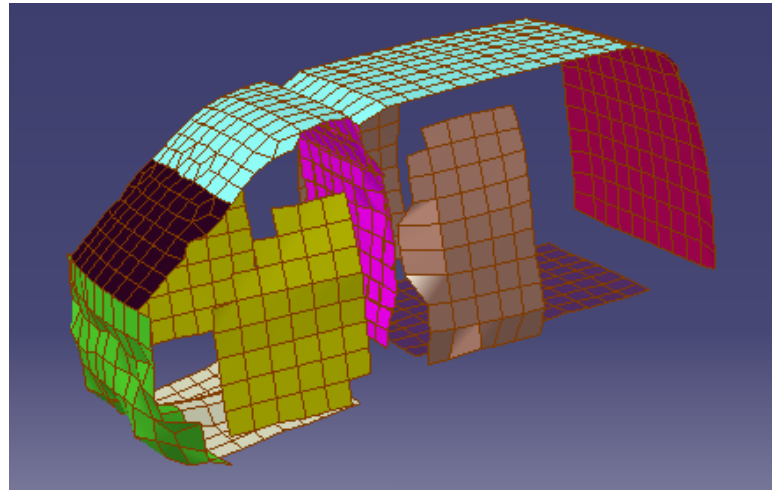


Figure 4.3 Panels on the cavity model

Totally 9 panels were created and their contributions to the sound pressure levels were obtained. In the following table, the names of the panels corresponding to different colors can be seen in table 4.1.

<b>COLOR</b>	<b>PANEL NAME</b>
Green	Front panel
Blue	Roof
Yellow	Front doors
White	Front floor
Pink	Bulkhead
Dark blue	Back floor
Red	Back panel
Dark brown	Window

Table 4.1 Panel names according to different colors

Similar to the uncoupled analyses, the module of data transfer was implemented to transfer the velocities. After that, field point mesh symbolizing the head of the driver was created and then ATVs were calculated. Finally, data transfer analysis results and ATVs were introduced and ATV response analysis was performed and the contribution of each panel was obtained (see figure 4.4).

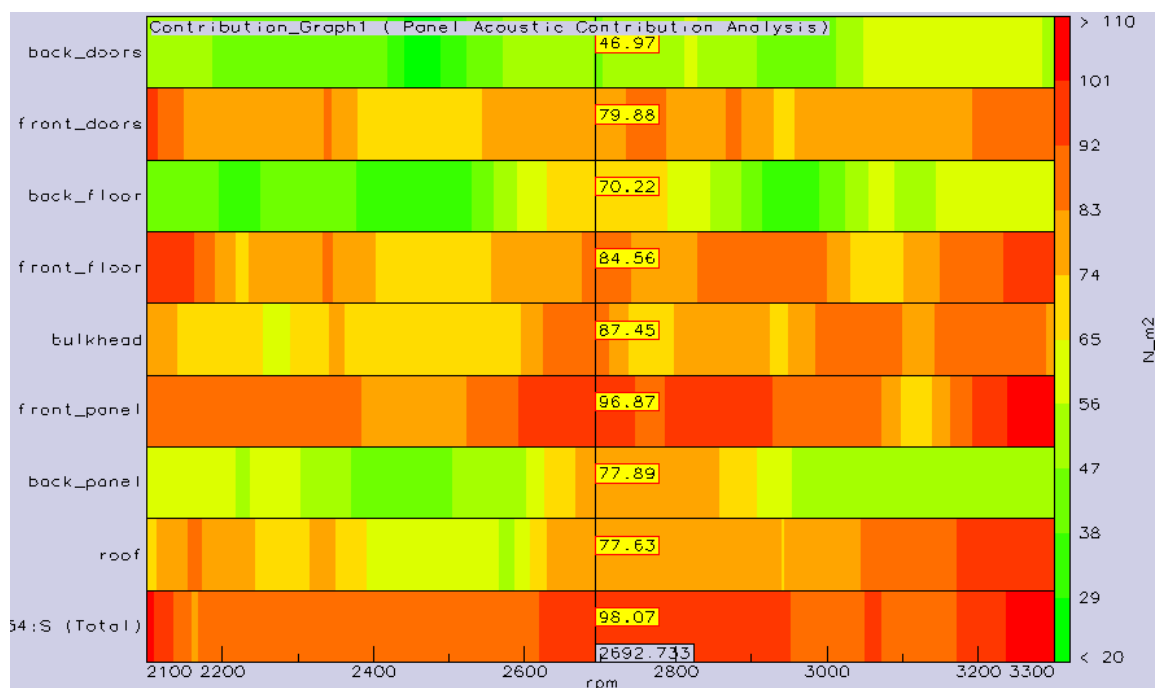


Figure 4.4 Panel Acoustic Contribution Analysis

Figure 4.4 shows the results of PACA. Red colored bars represent the least contribution and the yellow ones represent maximum contribution. According to Panel Acoustic Contribution Analysis, the most critical panels are front panel, bulkhead, front floors and front doors. The most significant panel is the front panel which contributes at all rpm values.



#### 4.1.2 Modal Acoustic Transfer Vector (MATV) Analysis

Modal Acoustic Transfer Vector analysis is another technique based on the ATV technology. MATV analysis is performed to find out which structural modes are affecting the sound pressure levels at the position of the driver's ear at most. Like PACA, MATV also integrates the FE model (structural mode) and the BE model (acoustic model) [26].

The structural response in equation (4.2) can be expressed as a linear combination of the mode shapes of the body, as in the following relation,

$$\{v_n(\omega)\} = j\omega[\phi_n]\{MRSP(\omega)\} \quad (4.4)$$

where  $[\phi_n]$  is the matrix composed of the modal vectors, projected on the local normal direction of the boundary surface, and  $\{MRSP(\omega)\}$  is the modal response (vector of the modal participation factors) of the structural model at a given excitation frequency.

Combining the equation (4.2) and equation (4.3) leads to

$$p(\omega) = \{ATV(\omega)\}^T j\omega[\phi_n]\{MRSP(\omega)\} \quad (4.5)$$

$$\text{Where } j\omega[ATM(\omega)]^T [\phi_n] = \{MATV(\omega)\}^T \quad (4.6)$$

is called the Modal Acoustic Transfer Vector (MATV), which can be directly combined with the modal response vector to give the sound pressure at a field point:

$$p(\omega) = \{MATV(\omega)\}^T \{MRSP(\omega)\} \quad (4.7)$$

MATVs express the acoustic transfer vector from the radiating structure to a field point in modal coordinates and therefore contain the acoustic contributions from each individual structural mode. The acoustic response in the field point is obtained by recombination of the MATV with the corresponding structural modal responses. Working in modal coordinates results in a significant data reduction. It's clear however that MATVs are no longer independent from the structural model as they are linked to the structural modal basis. Whenever the structural modal basis changes, e.g. due to structural design modifications, the set of MATV's needs to be reevaluated. From equation 6, it is clear that for a given structural modes set, the corresponding set of MATV's can easily be re-generated by projecting the ATV's, which are independent of the structural model as mentioned in section 4.1.1.1, into the modal space. It's important to note that this quick generation of MATV's by projecting the ATV's into a new modal basis is only valid if the acoustic configuration has not been changed due to the structural design modification [26].

As a result, acoustic pressure is obtained at the end of this analysis and can be represented as a color map on the field point mesh as seen below.

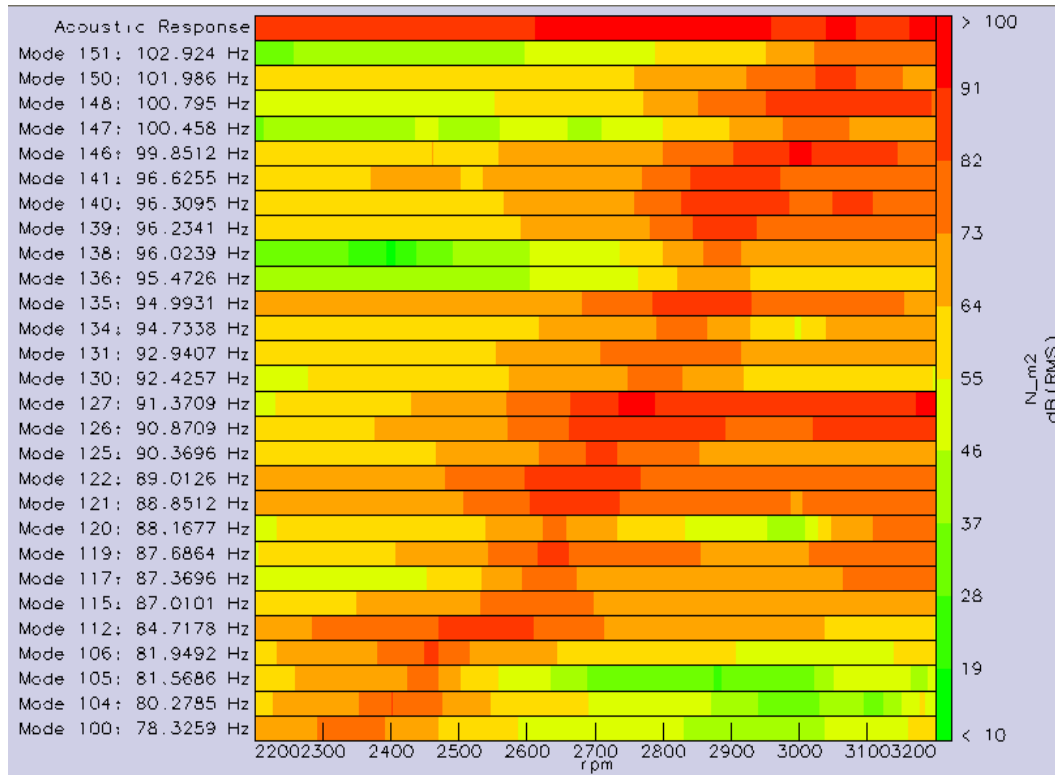


Figure 4.5 The contribution of structural modes to the acoustic response

In Figure 4.5, the yellow bars indicate the less contribution; red ones represent the maximum contribution. It is observed that modes 112, 121, 122, 126, 127 and 135 are very effective in a wide range of frequency.

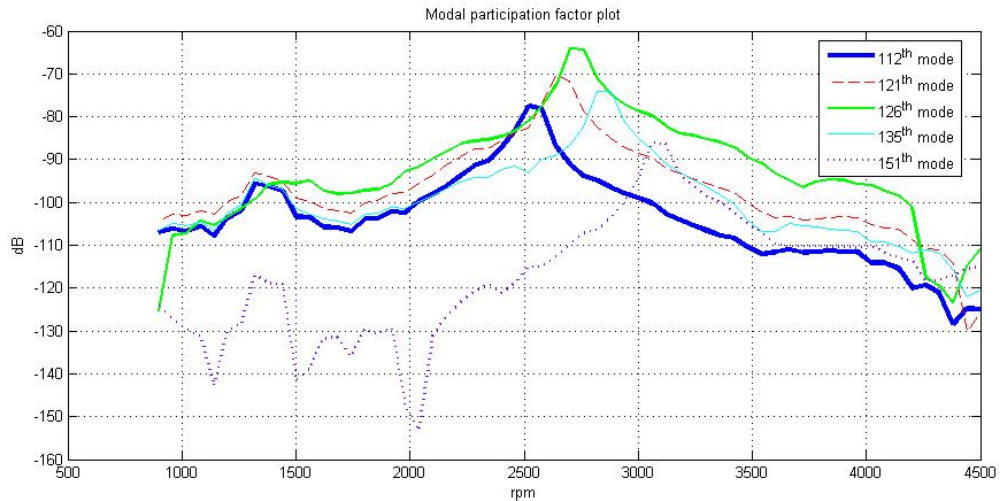


Figure 4.6 Modal Participation plot obtained from Modal-Based Force Response Analysis

Figure 4.6 shows the modal participation factors of these listed modes which are calculated by the Modal Based Force Response Analysis. Modal participation factors are not a clear indication of how these modes are coupled with the acoustical modes. However, figure 4.6 is helpful in determining the effective rpm range of each mode and also their relative magnitude with respect to each other.

#### 4.1.2.1 MATV Process Flow

The steps followed during MATV analysis are as the following:

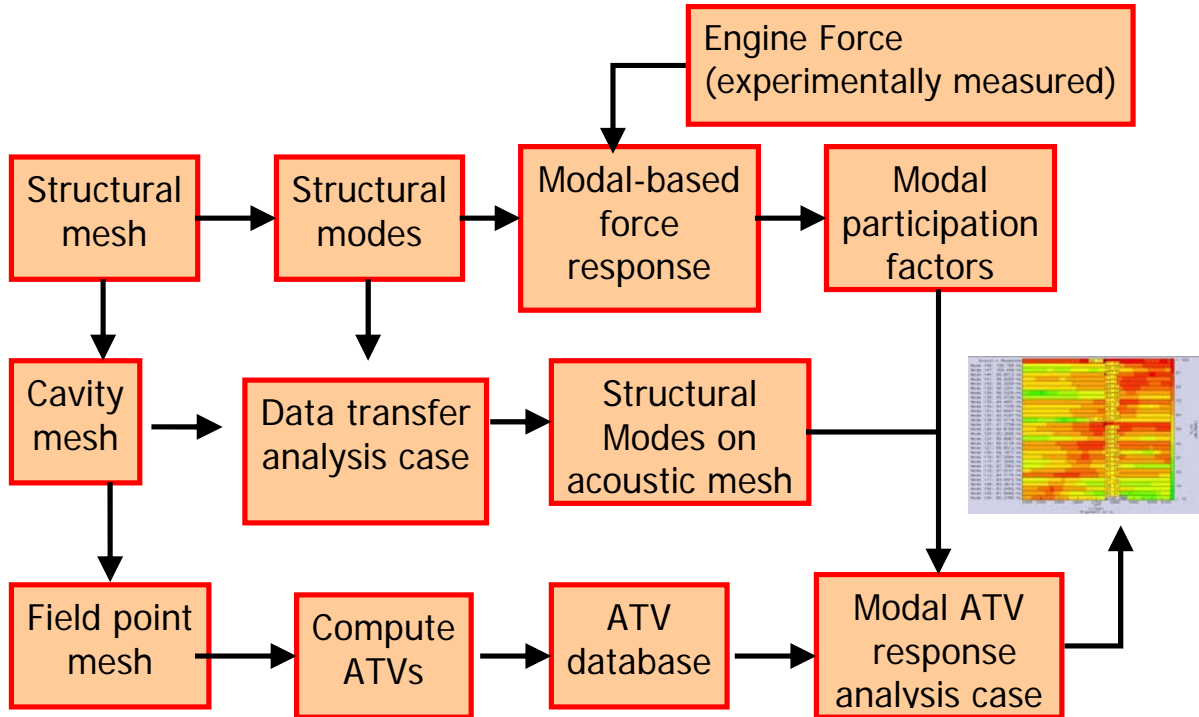


Figure 4.7 MATV Process Flow Diagram

As seen from the figure 4.7, some steps, such as performing structural analyses which include the calculation of structural modes and the harmonic analysis is the same with the PACA analysis. Different from PACA but similar to the coupled analysis, data transfer is performed to transfer the structural modes instead of panel velocities. Besides, modal participation factors gain importance in MATV analysis. Modal participation factors are obtained from the structural model and they do not include any information about the interaction between the structure and the cavity. Therefore, figure 4.6 can not give a final result about the contribution of structural modes. It can just give an idea why some modes are influential in a wide range of rpm values.

### **4.1.3 The evaluation of the results of PACA and MATV**

According to Modal Acoustic transfer Vector Analysis, modes 112, 121, 122, 126, 127 and 135 are very effective on the acoustic response in a wide range of frequency. The reason for this wide frequency range was investigated and explained via figure 34 obtained from Modal based force response analysis. In this figure, it can be seen that some modes make a sharp turn at their highest levels while some of them shows a horizontal behavior which means these modes contribute at most to the structural analysis at a wide range of frequency.

After determining the most significant modes, the related mode shapes were visualized to see which components have a significant deformation at these modes. It was found out that the left side of bulkhead and front panel were moving substantially in mode 112, whereas the front panel was one of the most moving panels in modes 126, 127 and 135. Also, maximum displacement occurs on the bulkhead in modes 121 and 122.

Finally, the results of Panel Acoustic Contribution Analysis were evaluated. According to Panel Acoustic Contribution Analysis, the most critical panels were identified as front panel, bulkhead, front floors and front doors. Especially the front panel and bulkhead are the most important panels contributing the most at all rpm values, which shows that MATV and PACA results are compatible with each other.

## Chapter 5

### APPLICATION OF THE HELMHOLTZ RESONATOR CONCEPT TO REDUCE THE SOUND PRESSURE LEVEL

In the previous chapters of this thesis, we performed vibro-acoustic analysis to predict the SPL in the passenger cabin of a commercial vehicle and then we have identified the problematic panels and calculated their contribution to the SPL by applying the ATV technology. In this chapter, we will apply the Helmholtz resonator (see figure 5.1) concept to reduce the SPL in the 80-100 Hz region. We generated a hole on the bulkhead of the vehicle such that the luggage compartment behaves as the cavity of the Helmholtz resonator whereas the hole can be considered as the neck of the resonator. The hole dimensions and locations on the bulkhead are altered to study the effect of the position and the neck size of the resonator.

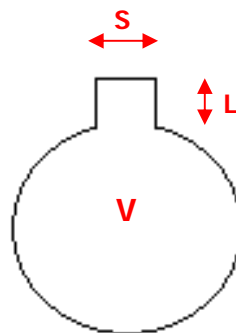


Figure 5.1 Helmholtz resonator

Helmholtz resonators are used in many applications to reduce the transmission of the unwanted sound [27]. They are commonly used to passively attenuate the noise in ducts. However, their attenuation is limited to single, narrow frequency bandwidth. Their attenuation frequency can be calculated by equation 5.1.

$$f = \frac{c}{2\pi} \sqrt{\frac{S}{VL}} \quad (5.1)$$

where  $c$ ,  $S$ ,  $L$ ,  $V$  represents respectively the sound speed, cross sectional area of the neck, effective length of the neck and cavity volume.

The Helmholtz resonators are widely used in industry to attenuate noise in various applications such as ducts and rocket fairings [27]. However, the literature about their application to reduce the noise inside the passenger cabins is very limited. Ahn et al. [28] presented an analytical method to investigate the structural-acoustic coupling characteristics of two cavities connected by small holes and in-between boundary structures. They used the definition of Helmholtz resonator to model these small holes.

Using multiple resonators with different natural frequencies can provide attenuation over a wide bandwidth. In addition to being limited to a single, narrow bandwidth, they have another drawback which is the limitation due to the volume constraints. Selamet and Lee [29] presented a study to eliminate this drawback. They focused on the effect of neck extension geometry on Helmholtz resonator behavior. They aimed to shift the resonance frequency without changing the volume.

There are some studies about the implementation of Helmholtz resonators to the rectangular enclosures instead of the ducts [30-33]. Fahy and Schofield [30] studied the interaction between a Helmholtz resonator and an acoustic mode of an enclosure. They



discussed the results of both free vibration and forced vibration. Cummings [31] investigated the effects of a resonator array on the cavity acoustic and developed a multi-mode theory for this purpose. He claimed that single-mode treatment became invalid if the modes are not well-separated in frequency. Pan et al. [32] studied the prediction of acoustic response in a rectangular enclosure but he took into account the types of boundaries like being damped due to some absorbent materials or having air leakage. Also the Helmholtz resonance effect of the cockpit in a helicopter was included. Following this study, Li and Cheng [33] proposed a similar study which is a direct expansion of Fahy and Scholfield's work to the case of multiple room modes coupled with multiple acoustic resonators and multiple sound sources. They also developed a multimode theory for describing the acoustic interaction between an enclosure and a Helmholtz resonator array.

Starting from the study of Kim and Lee [6] and benefiting from the use of Helmholtz resonator concept for noise attenuation which was explained in [30-33], we studied the effect of a hole on the bulkhead to reduce the unwanted sound in the vehicle. The location and the sizes of the holes are altered and then the acoustic response analyses were performed to see whether they cause an improvement on the SPL or not.

These analyses were done on a simple, rectangular model which has a mid-panel separating the cavity into two parts like in the car model. The geometry of the box model can be seen below and the material properties were represented in table 5.1.

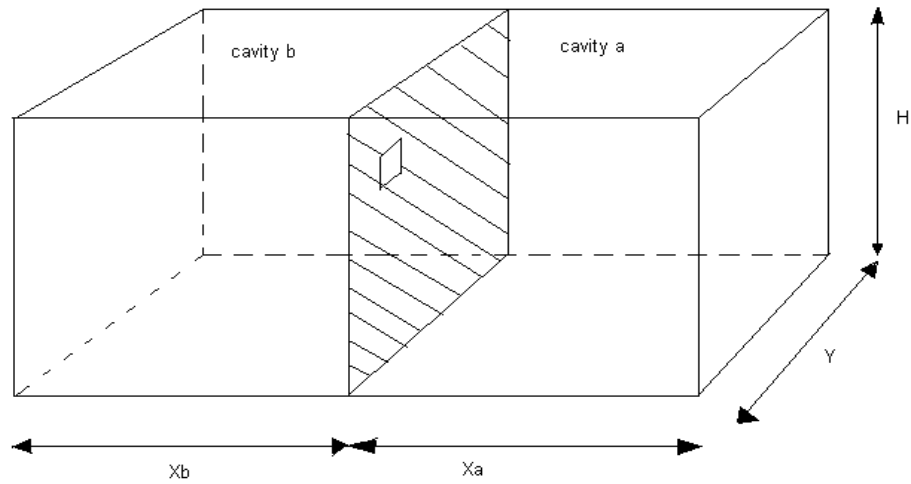


Figure 5.2 Three dimensional model for a rectangular box with a hole on the mid-panel

Cavity a	Cavity b	Mid-panel
$x_a = 0.86m$	$x_a = 0.110m$	<i>Young's modulus = 120GPa</i>
$Y = 0.36m$	$Y = 0.36m$	<i>Density = 7800kg / m<sup>3</sup>, Poisson ratio = 0.3</i>
$H = 0.30m$	$H = 0.30m$	<i>Thickness = 0.001m</i>

Table 5.1 Geometry and material data used for the simulation

For the beginning, the acoustic response analysis of the box model without a hole was performed and the sound pressure levels were obtained (figure 5.3)

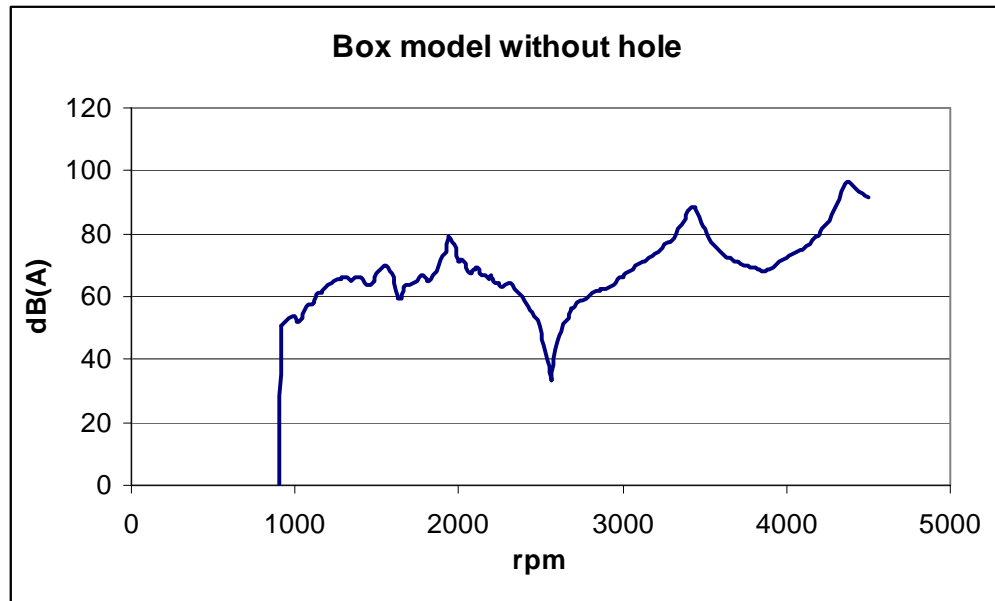


Figure 5.3 Sound pressure levels inside the box model

After that, holes were created separately on the mid-panel on different locations with the same size (30mmx30mm). The locations of these holes can be seen in the following figures. The circular area shows the location of the drivers head.

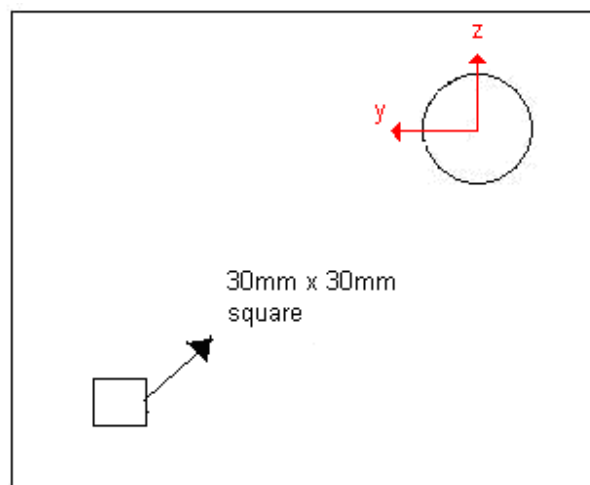


Figure 5.4 Model 1

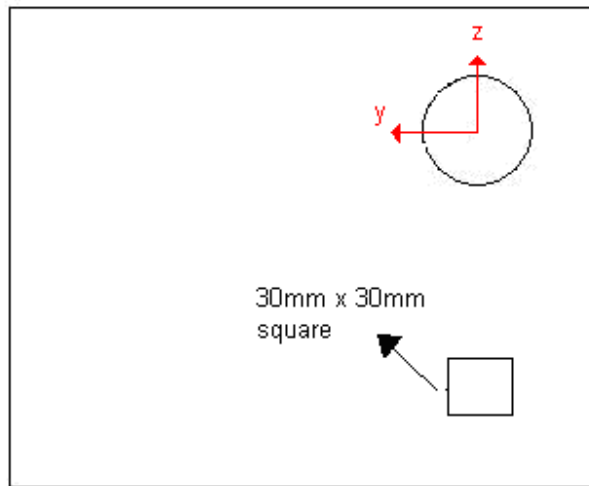


Figure 5.5 Model 2

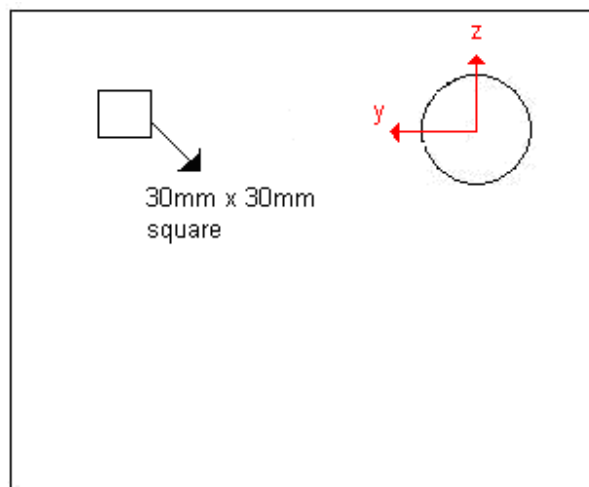


Figure 5.6 Model 3

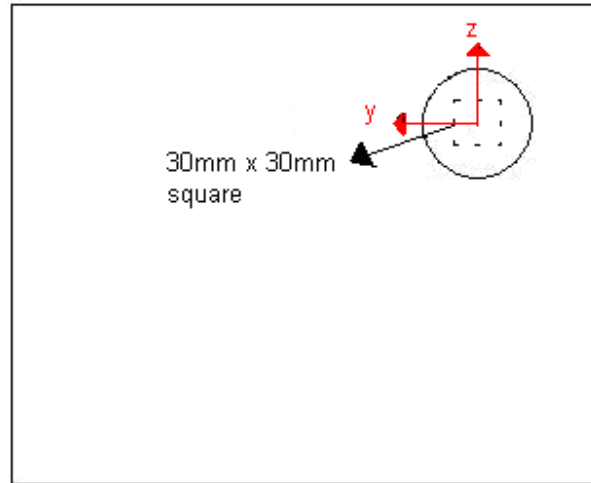


Figure 5.7 Model 4

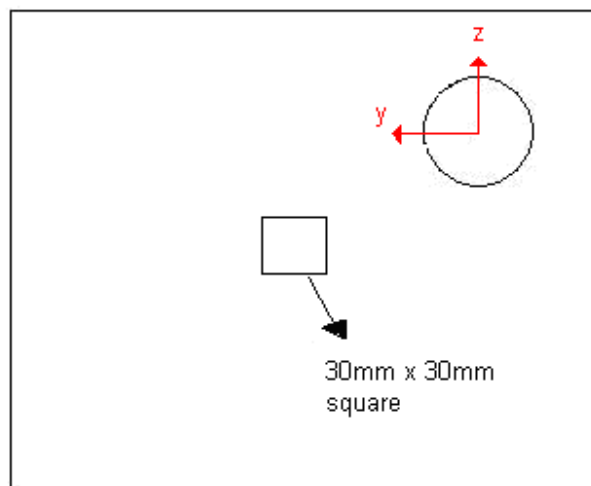


Figure 5.8 Model 5

The results of these analyses can be seen in figure 5.9. If we concentrate on the peak values, only the model 4 makes an improvement in the sound pressure levels around 3500 rpm. It was observed that it was the closest hole to the driver's ear compared to the other

ones. Other models make the noise levels worse around this rpm range. However, all the holes increase the dB values at the low rpm values between 1500-2000 rpm.

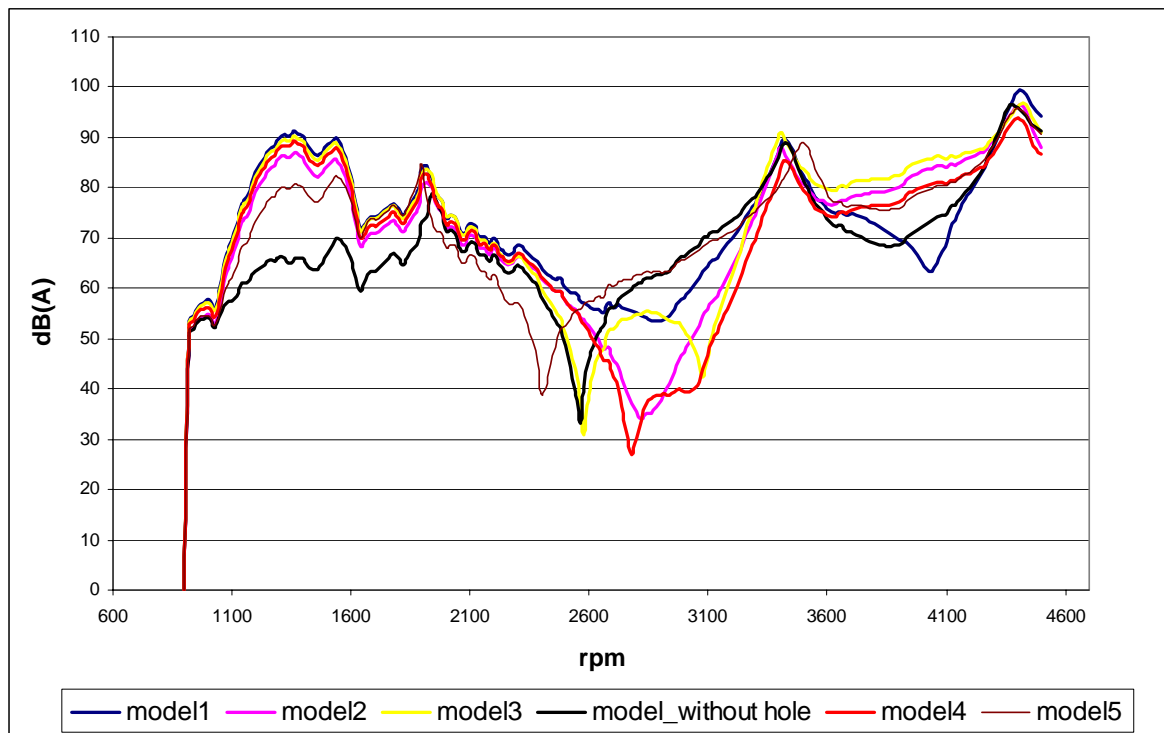


Figure 5.9 The sound pressure levels due to the different locations of holes

After determining the best location of the hole which provides a reduction in the sound pressure levels, the next analyses focused on changing the size of the hole. At first, the dimensions of the hole were changed as 50x50mm (model 4\_1). As a second solution, the location of 30x30mm hole was changed slightly in horizontal direction such that the hole gets closer to the ear location (model 4\_2). After changing the position of the hole horizontally, its dimensions were changed as 30x50mm such that it is stretched in the horizontal direction (model 4\_3).

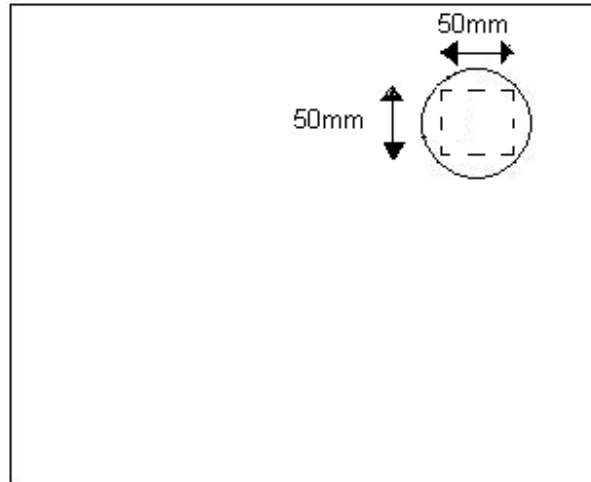


Figure 5.10 Model 4\_1

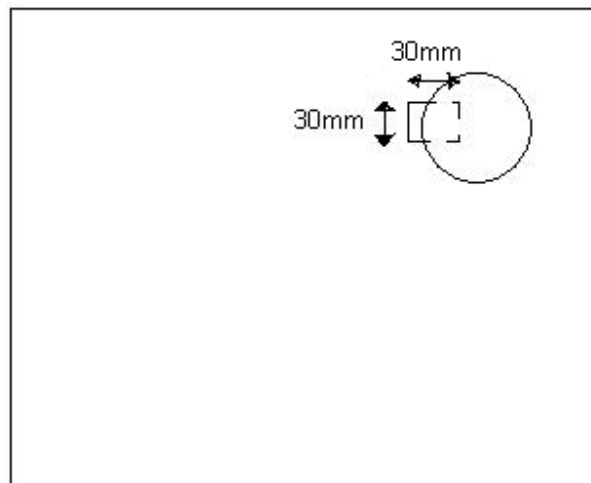


Figure 5.11 Model 4\_2

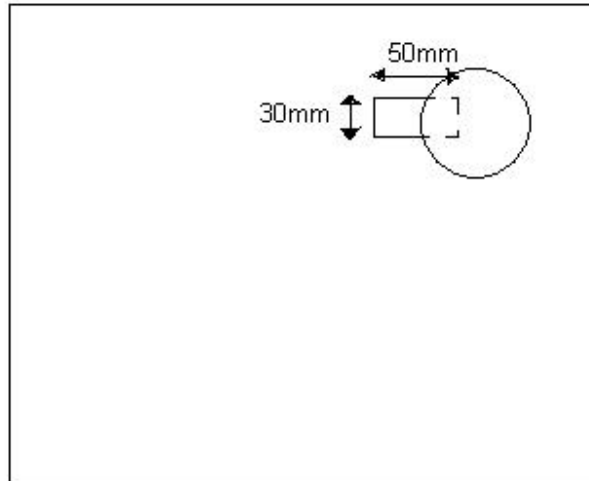


Figure 5.12 Model 4\_3

The results of the modifications which were done on the model 4 can be seen in Figure 5.13. According to this figure, model 4\_2 and model 4\_3 are the best combinations for the noise attenuation because they cause a reduction on the most significant SPL peaks not only at low frequencies around 2000rpm but also at higher frequencies around 3500rpm.



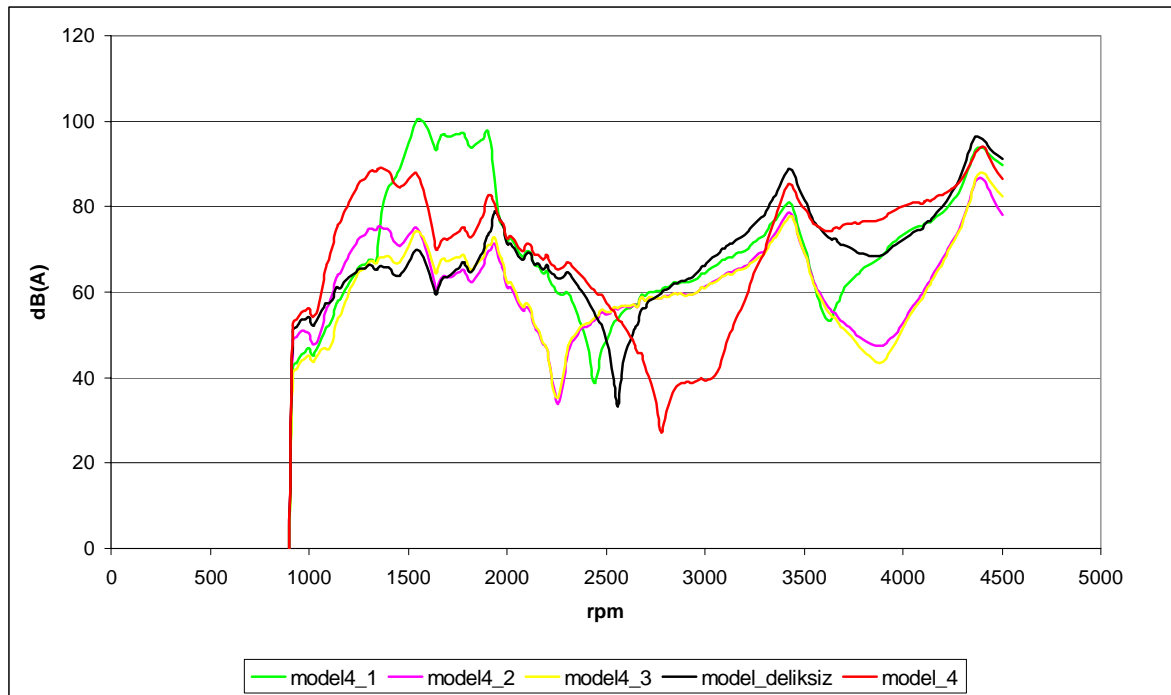


Figure 5.13 The sound pressure levels due to the modifications in model 4.

After these box analyses, the effect of a hole on the bulkhead was also investigated in our simplified car model. The hole was created only behind the driver's ear like model 4\_2 (see figure 5.11), because model 4\_2 makes an improvement in the sound pressure levels at more than one rpm value. That's why the hole behind the output point in the car model was also expected to reduce the sound pressure levels. Different from the box analyses, the output point was assigned as the left ear of the driver instead of the right ear. The result of the analysis can be seen in the following figure.

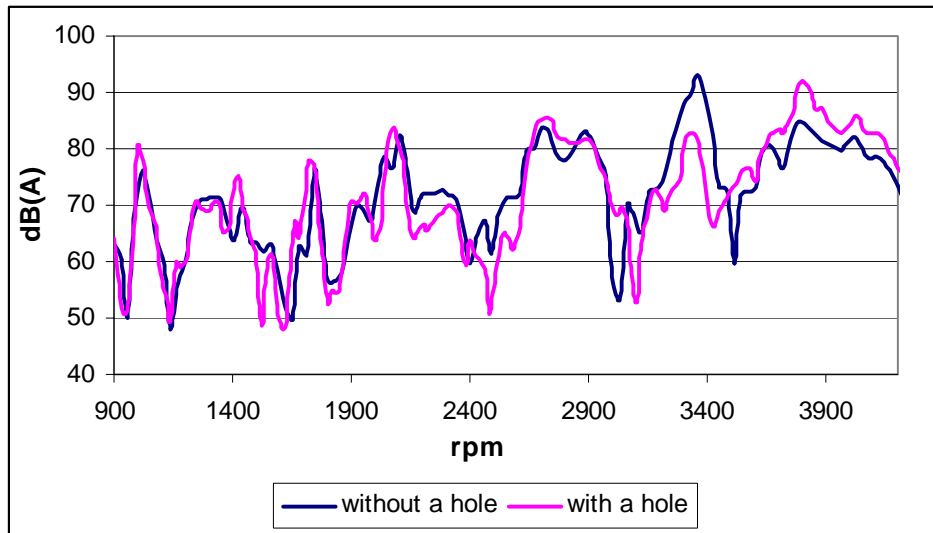


Figure 5.14 The effect of a hole on the bulkhead in the simplified structural model

According to figure 5.14, the hole makes an improvement around 3300 rpm. However, it makes SPL values worse between 2600rpm and 3000rpm, which is the frequency range of our concern. This result proves that a hole on the bulkhead behaves like a resonator, because it attenuates the unwanted noise in a certain and limited frequency range, while making the sound pressure levels worse at other rpm ranges.

After obtaining the sound pressure levels in the presence of a hole, the reason for the improvement occurred around 3300 rpm was investigated. For this purpose, MATV and PACA analyses were performed to see whether this hole changes the most contributing modes and panels of the car (see figure 5.15 and 5.16).

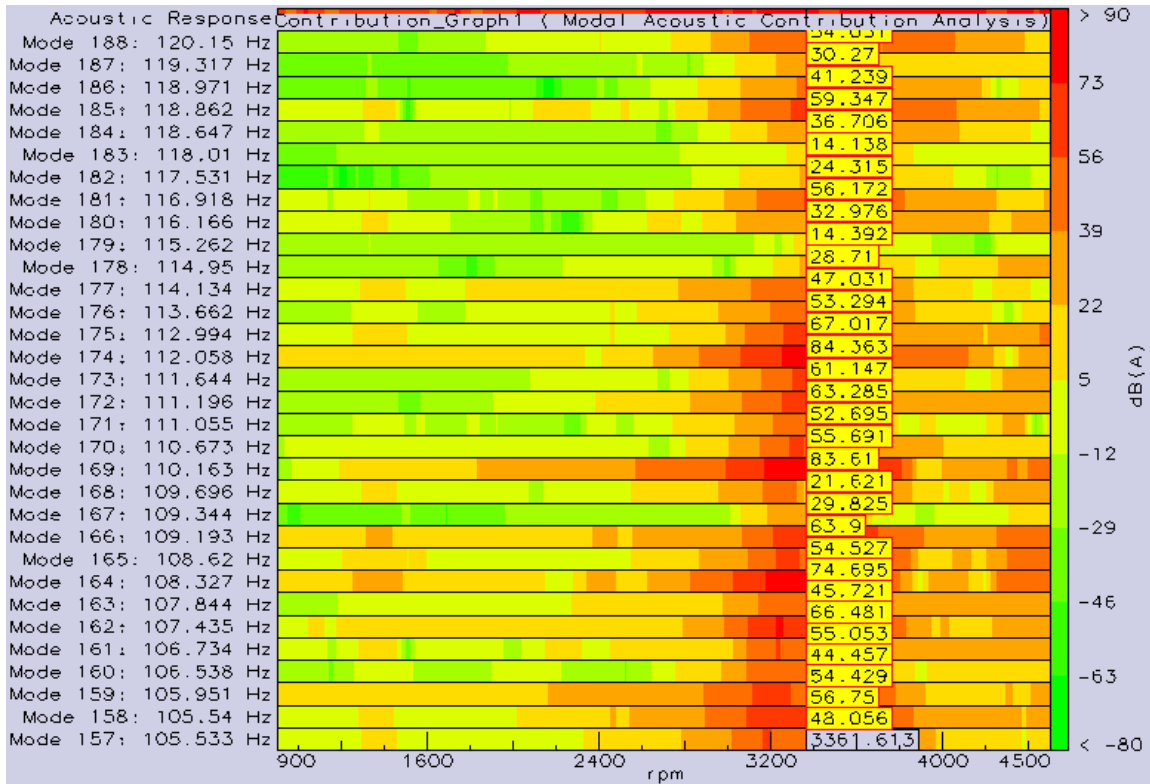


Figure 5.15 MATV results for the simplified structural model without a hole

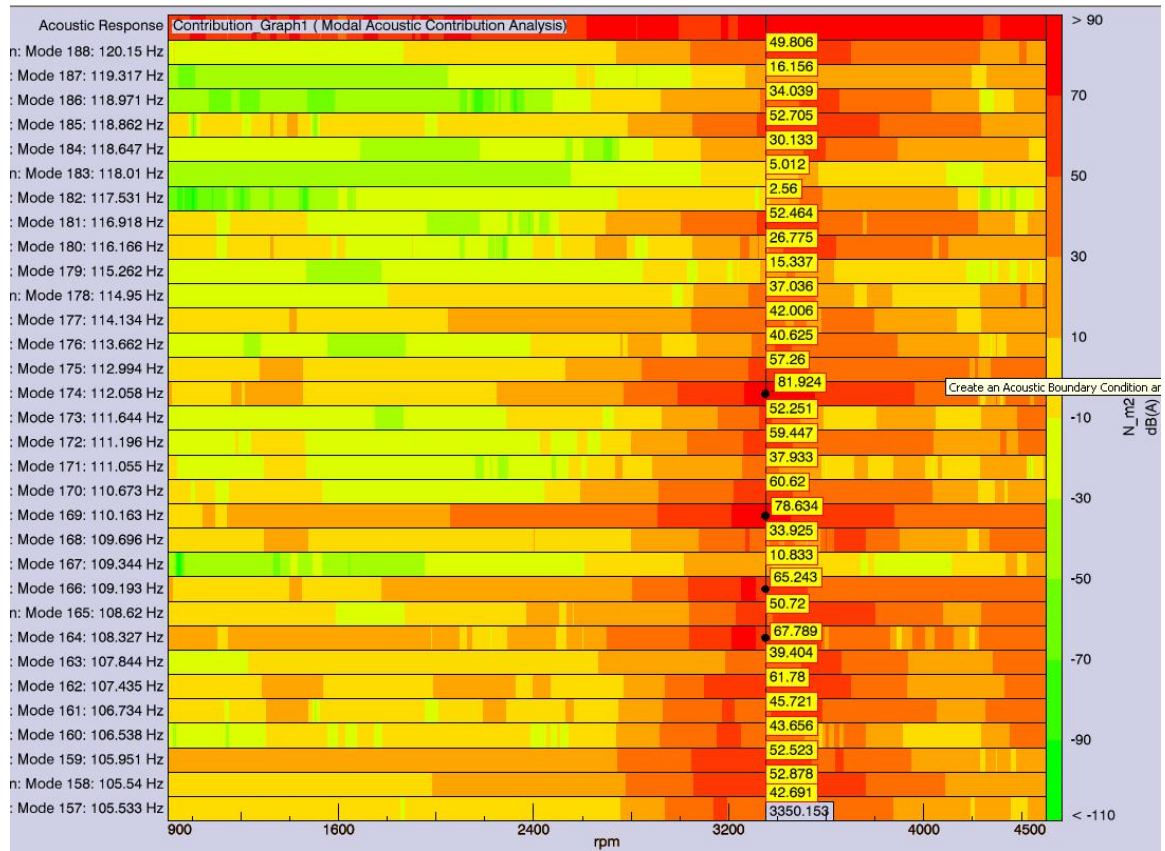


Figure 5.16 MATV results for the simplified structural model with a hole on the bulkhead

According to figure 5.15, the most contributing structural modes are mode 174 and 169. Their contribution rates are very close to each other, when there is no hole on the bulkhead. However, a hole on the bulkhead changes their contribution rates (see figure 5.16). Although the contribution of mode 174 does not change so much, the contribution of mode 169 decreases significantly and becomes the second influential structural mode on the acoustic response. This result gives us an idea that the decrease in the contribution of mode 169 may cause an improvement in the sound pressure levels.

After determining the change in the contributions of the structural modes, acoustic modal participation factors were visualized for both model with and without a hole (see figure 5.17 and 5.18).

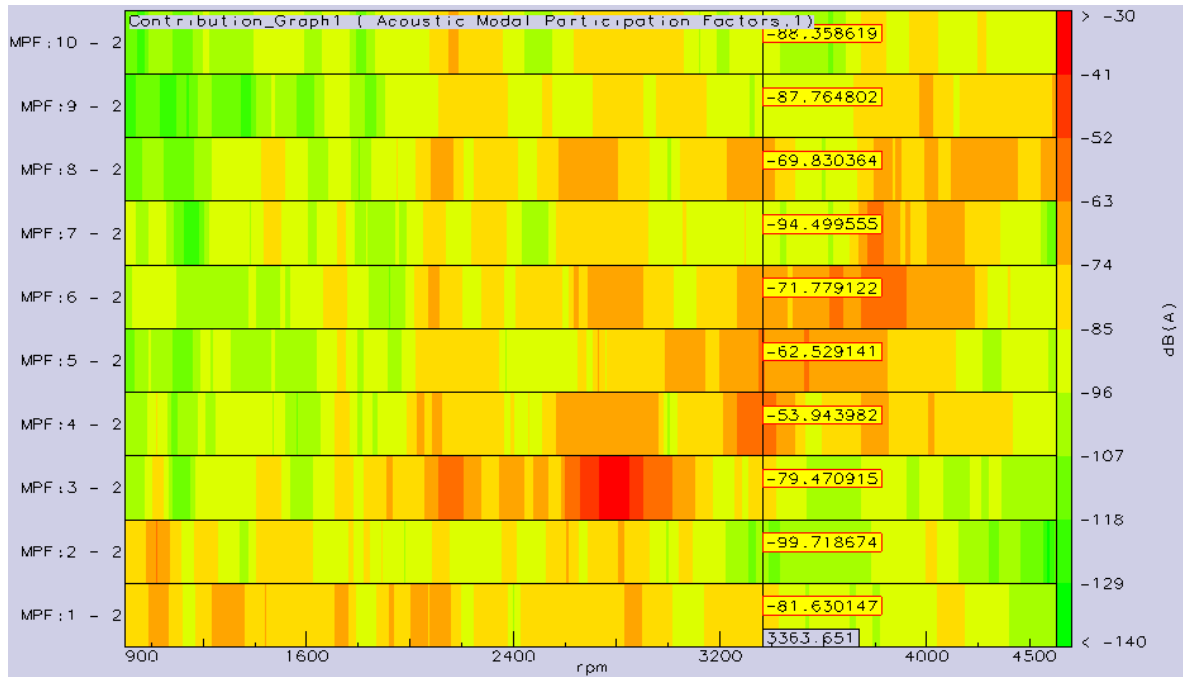


Figure 5.17 Acoustic modal participation factors for the model without a hole

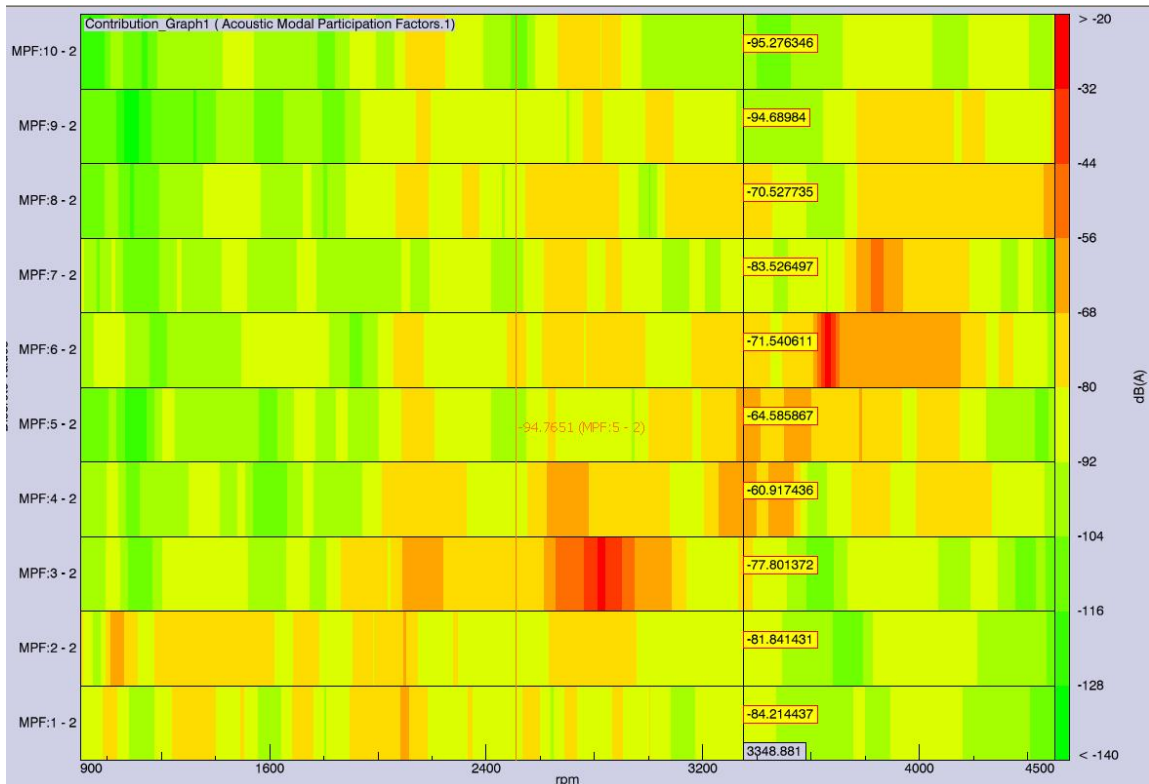


Figure 5.18 Acoustic modal participation factors for the model with a hole

According to figure 5.17 and 5.18, the most influential acoustical modes are the 4<sup>th</sup> and 5<sup>th</sup> modes around 3300 rpm. When there is a hole on the bulkhead, the contribution of 4<sup>th</sup> mode decreases and comes closer to the contribution of the 5<sup>th</sup> mode. Therefore, it can be said that the structural mode 169 and the 4<sup>th</sup> acoustic mode is normally coupled with each other, and this hole breaks down their coupling such that the sound pressure levels are attenuated.

The following figures show the results of Panel Acoustic Contribution Analyses. According to these figures, the contribution rates of panels does not change in the presence

of a hole, but total dB(A) value decreases from 91dB(A) to 82 dB(A), which means almost 10% reduction in the sound pressure level.

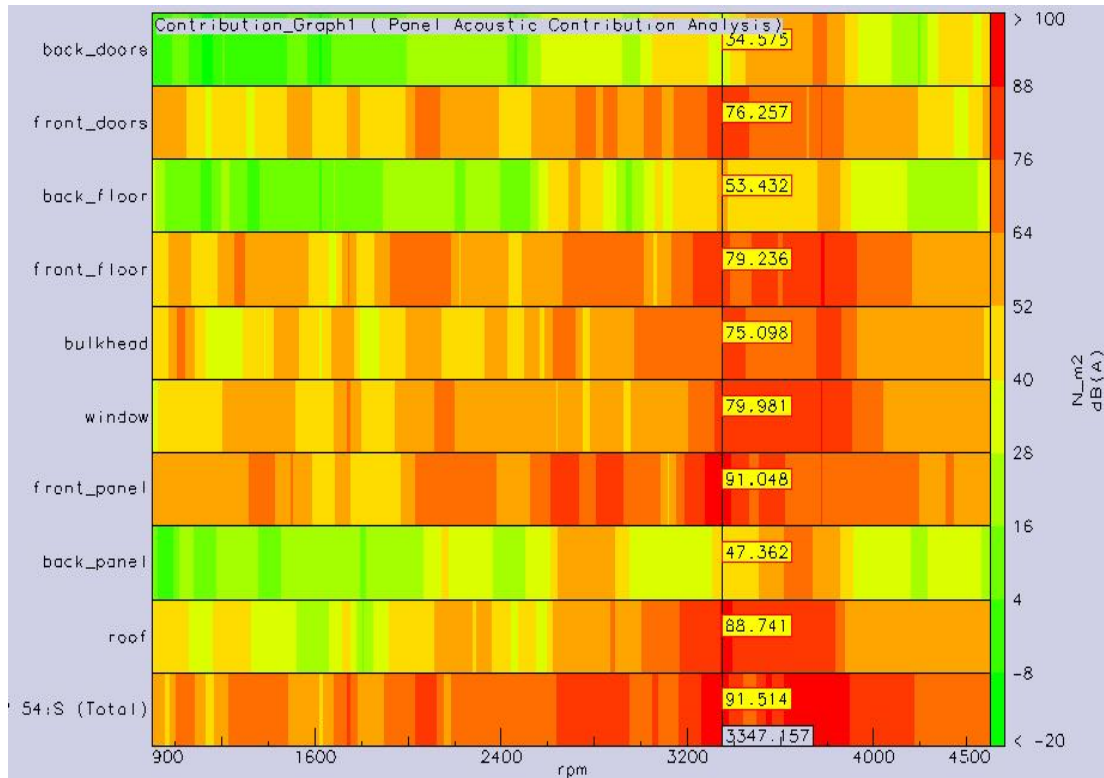


Figure 5.19 The result of Panel Acoustic Contribution Analysis without a hole

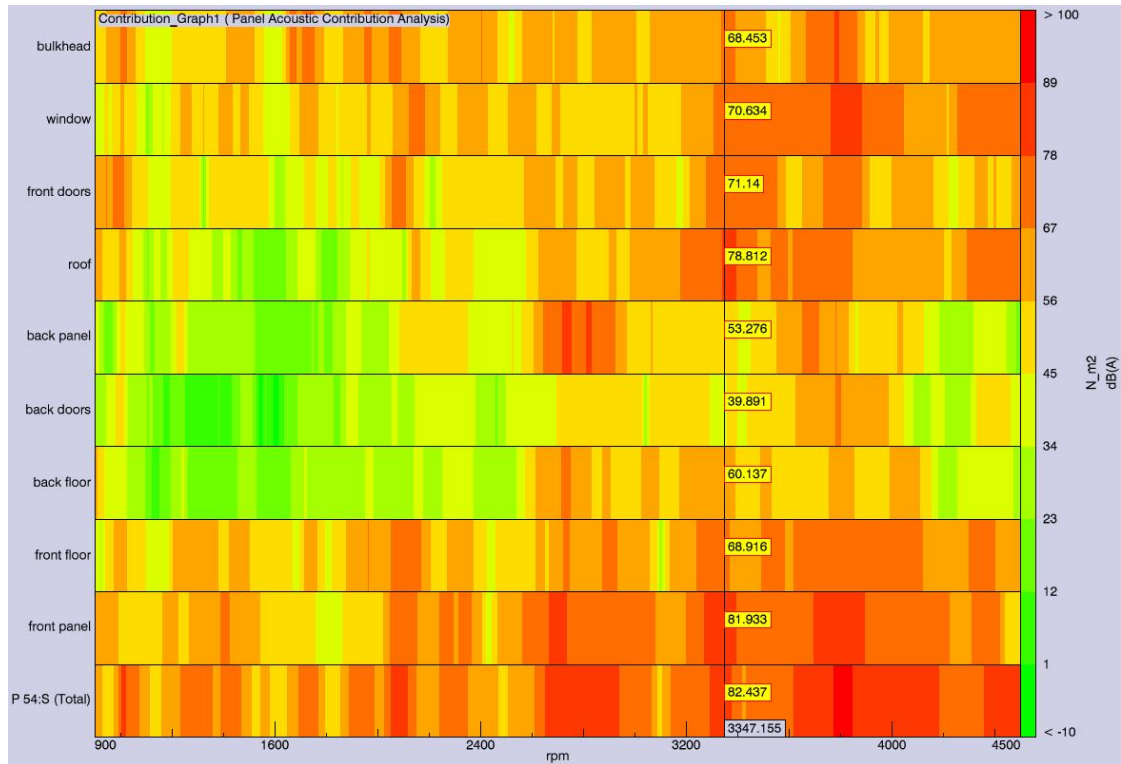


Figure 5.20 The result of Panel Acoustic Contribution Analysis with a hole



## Chapter 6

### DISCUSSION AND CONCLUSION

In this study, we developed a systematic approach to predict and also improve the structure-borne noise which is mainly caused by the vibrating panels enclosing the vehicle. The developed approach utilizes a combined FEM/FEM and FEM/BEM methodology to predict the SPL in a passenger cabin of a vehicle. The transfer paths of the disturbances coming from the engine and the most significant structural modes and panels can be identified with the presented approach. After the critical panels that contribute to the SPL are identified, new improvements and design modifications can be performed on the vehicle to reduce the sound pressure levels.

In Chapter 3, we performed the traditional FEM/FEM analysis to understand whether we should use the coupled or uncoupled analysis to predict the cabin sound pressure levels. In the coupled method, there is a mutual interaction between the structure and the cavity whereas the interaction is one way in the uncoupled analysis. The comparison of coupled and uncoupled analysis show that the cabin SPL can be predicted by uncoupled analysis accurately and this method was used to determine the most critical engine mounts because it is computationally less expensive when it is compared to the coupled analysis. The most effective disturbance transfer paths were identified. The transfer functions or in other words the SPL under the effect of 1 N force were compared with the measured ones in all disturbance directions. It was observed that the model predictions were not that accurate because of the simplifications made in the structural model. The disturbance amplitudes

were scaled such that the SPL predictions were in the same order of magnitude with the experimentally measured ones.

In Chapter 4, FEM/BEM methodology is used to identify the sources of the high peaks in the SPL performance. The FEM/BEM methodology benefits from a new technology called “ATV (Acoustic Transfer Vector) technology”, which allows two detailed analyses called Modal Acoustic Transfer Vector (MATV) and Panel Acoustic Contribution Analysis (PACA). MATV algorithm allows the calculation of acoustic contribution of each individual structural mode, and PACA enables the user to determine the contribution rate of each radiating panel to the noise level inside the cabin. These two analyses are much more efficient in predicting the sound pressure levels for complex problems than the other traditional FEM/FEM approach. The traditional FEM/FEM approach uses the structural vibrations directly to define the boundary conditions for the acoustic radiation problem. However, ATVs are independent of loading, and structural velocities (indirectly loading) are introduced to the model as the boundary conditions. In addition, ATVs doesn't change even if velocities vary due to different loading conditions, because ATVs are dependent only on the geometry of the acoustic domain, the frequency and the location of the output field points.

The structural modes 112, 121, 122, 126, 127 and 135 were identified as the most effective structural modes around 2700 rpm by the MATV analysis. The results of PACA showed that the front panel is the most contributive panel to the SPL at all rpm range. However, other panels such as bulkhead and front floor were also found to be significant in contribution to the acoustic response.

Finally, the idea of using a Helmholtz resonator in the cabin was studied to reduce the sound pressure levels. A hole is placed on the bulkhead of the vehicle to make it behave as a Helmholtz resonator such that the luggage compartment behaves as the cavity of the Helmholtz resonator whereas the hole can be considered as the neck of the resonator. The hole dimensions and locations on the bulkhead are altered to study the effect of the position and the neck size of the resonator. First, the analysis was performed on a simple rectangular box to determine the optimum location and size of the hole. Then, the analysis was repeated on the vehicle model that was used throughout this thesis. The results show that the hole on the bulkhead behaves as a Helmholtz resonator and improves the SPL at certain frequencies. However, it introduces another cavity mode and this additional mode can make the SPL worse at other frequencies.

For the future work, other ways of reducing the interior noise can be investigated. For example, the design parameters of the radiating panels (i.e., thickness, damping, and material) with highest levels of contribution rates can then be optimized or structural absorbers can be mounted onto the identified critical engine mounts.

**BIBLIOGRAPHY**

- [1] Lalor, N. and Priebisch, H-H., "The prediction of low- and mid-frequency internal road vehicle noise: a literature survey." *J. Automobil Engineering*, 221, 245-269, 2007
- [2] Desmet W., and Sas P., "Introduction to Numerical Acoustics" *LMS Numerical Acoustics Theoretical Manual*, 5-35.
- [3] Dowell E. H., "Master Plan for Prediction of Vehicle Interior Noise" *AIAA Journals*, 18(4), 353-366, 1980.
- [4] Dowell, E. H., and Voss, H. M., "The Effect of a Cavity on Panel Vibration" *AIAA Journals*, 1(2), 476-477, 1963.
- [5] Dowell, E.H., Gorman, G.F., III, and Smith, D.A., "Acoustoelasticity: General Theory, Acoustic Natural Modes and Forced Response to Sinusoidal Excitation, Including Comparisons With Experiment," *J. Sound and Vib.*, 52(4), 519-542, 1977.
- [6] Kim S.H., Lee J.M., and Sung M. H., "Structural-Acoustic Model Coupling Analysis and Application to Noise Prediction in a Vehicle Passenger Compartment" *Journal of Sound and Vibration*, 225(5), 989-999, 1999.
- [7] Kim S.H., and Lee J.M., "A Practical Method for Noise Reduction of a Vehicle Passenger Compartment" *Journal of Vibration and Acoustics*, 120,199-205, 1998.
- [8] Suzuki S, Maruyama S, Ido H. "Boundary element analysis of cavity noise problems with complicated boundary conditions." *J Sound and Vibr*, 130(1), 79-91, 1989.
- [9] Freymann R, Stryczek R, Spannheimer H. "Dynamic response of coupled structural-acoustic systems." *J. Low Frequency Noise Vibr*, 14(1), 11-32, 1995.
- [10] Pal C, Hagiwara I., "Dynamic analysis of a coupled structural-acoustic problem. Simultaneous multimodal reduction of vehicle interior noise level by combined optimization." *Finite Elements Anal Des*, 14, 225-34, 1993.
- [11] Nefske D. J., Wolf J. A., and Howell L. J., "Structural -acoustic finite element analysis of the automobile passenger compartment: a review of current practice" *Journal of Sound and Vibration*, 80(2), 247-266, 1982.

- 
- [12] Marburg S, Hardtke HJ., “A study on the acoustic boundary admittance. Determination, results and consequences.” *Eng Anal Boundary Elements*, 23, 737–44, 1999.
- [13] Marburg S, Hardtke H-J., “Shape optimization of a vehicle hat-shelf: improving acoustic properties for different load cases by maximizing first eigenfrequency.” *Comput Struct.*, 79(20–21), 1943–57, 2001.
- [14] Marburg S, Beer H-J, Gier J, Hardtke H-J. “Experimental verification of structural-acoustic modelling and design optimization.” *J Sound and Vibr*, 252(4), 591–615, 2002.
- [15] Marburg S. “Efficient optimization of a noise transfer function by modification of shell structure geometry – Part I: Theory.” *Struct Multidisciplinary Optim*, 24(1), 51–9, 2002.
- [16] Marburg S, Hardtke H-J. “Efficient optimization of a noise transfer function by modification of shell structure geometry – Part II: Application to a vehicle dashboard.” *Struct Multidisciplinary Optim.*, 24(1), 60–71, 2002
- [17] Vlahopoulos N. “Numerical structure-borne noise prediction scheme based on the boundary element method with a new formulation for the singular integrals.” *Comput Struct*, 50(1), 97–101, 1994
- [18] Liu, Z. S., Lu, C., Wang, Y. Y., Lee, H. P., Koh, Y. K., Lee, K. S. “Prediction of noise inside tracked vehicle.” *J Applied Acoustics*, 64, 74-91, 2006.
- [19] Bregant, L., Miccoli, G., Seppi, M. “Construction machinery cab vibro-acoustic analysis and optimization, <http://www.femtools.com/download/docs/nafems05c.pdf>
- [20] Citarella R., Federico L., and Cicatiello A., “Modal acoustic transfer vector approach in a FEM–BEM vibro-acoustic analysis” *Engineering Analysis and Boundary Elements*, 31, 248-258, 2007.
- [21] Desmet W., and Vandepitte D., “Finite Element Modeling for Acoustics” *LMS Numerical Acoustics Theoretical Manual*, 37-85.

- 
- [22] Desmet W., “Boundary Element Modeling for Acoustics” LMS Numerical Acoustics Theoretical Manual, 86-126.
- [23] Pirk R., Desmet W., Pluymers B., Sas P., and Goes L., “Vibro-acoustic Analysis of the Brazilian Vehicle Satellite Launcher (VLS) fairing” Proceedings of ISMA 2002, 5, 2075-2084.
- [24] Alia A. and Souli M., “Acoustic and Vibroacoustic Modelling in LSDYNA based on Variational BEM” 5<sup>th</sup> European LS-DYNA Conference, 4c-62.
- [25] Herrin D. W., Martinus F., and Seybert A. F., “Using Numerical Acoustics to Diagnose Noise Problems” SAE Technical Paper Series, 2005-01-2324.
- [26] Tournour M., “ATV Concept and ATV based applications” LMS Numerical Acoustics Theoretical Manual, 127-139.
- [27] Griffin S., Lane S.A., and Huybrechts S., “Coupled Helmholtz Resonators for Acoustic Attenuation” Journal of Vibration and Acoustics, 123, 11-17, 2001.
- [28] Ahn C.G., Choi H.G., and Lee J.M., “Structural-Acoustic Coupling Analysis of Two Cavities Connected by Boundary Structures and Small Holes” ASME, 127, 566-574, 2005.
- [29] Selamet A., and Lee L., “Helmholtz resonator with extended neck” Journal of Acoustical Society of America, 113(4), 1975-1985, 2003.
- [30] Fayh F. J., and Schofield C., “A note on the interaction between a Helmholtz resonator and an acoustic mode of an enclosure” Journal of Sound and Vibration, 72(3), 365-378, 1980.
- [31] Cummings A., “The effects of a resonator array on the sound field in a cavity” Journal of Sound and Vibration, 154(1), 25-44, 1992.
- [32] Pan J., Elliott S. J., and Baek H. H., “Analysis of low frequency acoustic response in damped rectangular enclosure” Journal of Sound and Vibration, 223(4), 543-566, 1999.
- [33] Li D., and Cheng L., “Acoustically coupled model of an enclosure and a Helmholtz resonator array” Journal of Sound and Vibration, 305, 272-288, 2007.

### VITA

Gülşen Kamçı was born in Bursa, Turkey, on March 18, 1984. She received her B.Sc. Degree in Mechanical Engineering from Istanbul Technical University, Istanbul, in 2006. From September 2006 to September 2008 she worked as teaching and research assistant at Koç University, Istanbul, Turkey. She has worked on “Vibro-Acoustic Modeling of a Commercial Vehicle to Reduce the Interior Noise Level” during her M.S. study. During her research study, she submitted two conference papers, titled “Investigating the Sound Pressure Level inside the Passenger Cabin of an Automobile using a Vibro-Acoustic Model” and “Vibro-Acoustic Modeling of a Commercial Vehicle to Reduce the Interior Noise Level”. She attended INTERNOISE 2008 (Shanghai, China) where she presented her second paper.